

# Unidimensional models of acoustic propagation in axisymmetric waveguides

Thomas Hélie<sup>a)</sup>

*IRCAM, Centre G. Pompidou, CNRS UMR 9912, Équipe Analyse-Synthèse, 75004 Paris, France*

(Received 8 November 2002; revised 25 June 2003; accepted 21 July 2003)

This paper presents a model of the linear acoustic propagation in axisymmetric waveguides, the pressure depending on a single space variable. The approach consists of writing the wave equation and the boundary conditions for a coordinate system rectifying the isobaric map at each time. The two-dimensional dependence of the problem is thus transferred from the pressure to the coefficients of the wave equation. From this result, an exclusively geometrical necessary condition is deduced for the admissibility of isobaric maps. However, the knowledge of the waveguide geometry is not sufficient to separate the pressure and the isobaric map solutions. In order to develop a unidimensional wave equation, a geometrical hypothesis is discussed. For lossless and motionless rigid waveguides, the deduced equation leads to exact results for tubes and cones. It may be interpreted as a Webster equation for a particular coordinate system so that the particular profiles for which analytical solutions of the pressure exist are redefined. The wave equation is also established for pipes with visco-thermal losses and, more generally, for mobile walls having a small admittance. The compatibility of the geometrical hypothesis with the exact model is specified for this general case. © 2003 Acoustical Society of America. [DOI: 10.1121/1.1608962]

PACS numbers: 43.20.Mv, 43.20.Bi [MO]

Pages: 2633–2647

## I. INTRODUCTION

This work derives models accounting for acoustic propagation in axisymmetric waveguides and which depend on a single spatial variable. Such models are interesting because of their compactness of description which reveals the main effect involved in the variation of the cross section. For the same reason, they are also well adapted to the derivation of low-cost numerical simulations. The first establishment of such one-dimensional (1D) models is due to Bernoulli<sup>1</sup> and Lagrange,<sup>2</sup> even if the corresponding equation is commonly mentioned as the Webster equation.<sup>3</sup> This equation has been extensively investigated, as witnessed by the bibliography compiled by Eisner,<sup>4</sup> and the various geometrical hypotheses used for its derivation have been periodically discussed. Thus, planar wavefronts were contested by Lambert<sup>5</sup> and Weibel<sup>6</sup> who postulated spherical and curved ones, respectively. They reported the inadequacy of the first assumption, exhibiting the fact that wavefronts may be orthogonal to any curved rigid wall. The quasisphericity was experimentally confirmed for a horn profile in the low frequency range by Benade and Jansson.<sup>7</sup> Later, Putland<sup>8</sup> looked for necessary and sufficient conditions for a propagative acoustic mode to be spatially dependent on a single parameter. He pointed out that one-parameter acoustic fields obey a Webster equation and exhibited parallel planes, coaxial cylinders, and concentric spheres as the only possible corresponding potential surfaces. Nevertheless, even if finding a general 1D model is hopeless and leads to other approaches,<sup>9–11</sup> the simplicity of the Webster equation still stimulates the search for more accurate 1D models. Thus, Agulló, Barjau, and Keefe<sup>12</sup> re-

cently assumed the time-invariance of equipotential surfaces and developed 1D models for both spherical and oblate ellipsoidal surfaces.

In this paper, a local geometrical hypothesis is proposed, namely, the quasi-sphericity of isobars near the wall. This hypothesis agrees with Benade and Jansson's experiment<sup>7</sup> but does not require the wavefronts to be fixed. The general method relies on a time-domain wave equation established for a coordinate system locally rectifying the isobaric map at each time. The rectification ensures that the pressure is reduced to a 1D function, but, concurrently, it transfers the two-dimensional (2D) dependence of the pressure to the coefficients of the isobaric wave equation. Establishing 1D models requires making an assumption. The quasisphericity hypothesis is chosen as a natural extension of the property satisfied by plane and spherical waves travelling in cylinders and cones, respectively. Moreover, it does not resort to integral equations or averaging operators as usual, and makes the rectification method able to treat the case of rigid immobile walls as well as that of moving walls with a small admittance.

The structure of the paper is as follows: Sec. II presents the problem. Section III establishes all the exact derivations. General geometrical definitions are presented. The wave equation is expressed in a coordinate system which locally rectifies the isobaric map at each time. An admissibility condition necessarily satisfied by any isobaric map is then deduced. The case of static isobaric maps is investigated. Section IV develops a 1D model for rigid motionless walls. The geometrical hypothesis is first detailed. The derived 1D model is proven to be equivalent to the Webster equation for which the longitudinal coordinate measures the arc length of the wall. The validity of both the hypothesis and the model is discussed. The particular profiles for which analytical solu-

<sup>a)</sup>Electronic mail: thomas.helie@ircam.fr; Université de Paris XI-Orsay, Paris, France.

TABLE I. List of symbols.

$\rho_0$	density of air
$c$	speed of sound in air
$\begin{cases} z=f(s,u,t) \\ r=g(s,u,t) \end{cases}$	time-varying change of spatial coordinates
$p(z,r,t), \tilde{p}(s,u,t)$	acoustic pressure located at $(z,r,t)$ and $(s,u,t)$ , respectively
$\mathbf{v}(z,r,t)$	particle acoustic velocity located at $(z,r,t)$
$\mathcal{I}_{s,t}$	isobars indexed by $s$ at the time $t$
$\mathcal{I}_{u,t}$	axisymmetric surfaces indexed by $u$ at the time $t$
$\mathcal{W}_t$	wall of the guide at the time $t$
$q _w(s,t)$	quantity $q(s,u,t)$ evaluated in $u=w$ i.e. on $\mathcal{I}_{w,t}$
$\mathbf{u}_z, \mathbf{u}_r$	unit vectors associated with the longitudinal ( $z$ ) and the transverse ( $r$ ) coordinates of the cylindrical basis
$\mathbf{u}_s(s,u,t), \mathbf{u}_u(s,u,t)$	field of unit vectors tangent to $\mathcal{I}_{s,t}$ and $\mathcal{I}_{u,t}$ , respectively
$\mathbf{w}_s(s,u,t), \mathbf{w}_u(s,u,t)$	vectors $\mathbf{u}_s(s,u,t)$ and $\mathbf{u}_u(s,u,t)$ rotated from $+\pi/2$
$\sigma_s(s,u,t), \sigma_u(s,u,t)$	norms of the vectors of the basis induced by the change $(f,g)$ for the coordinates $s$ and $u$ , respectively
$\xi_s(s,u,t), \xi_u(s,u,t)$	Mach numbers of a point located at $(s,u)$ for the orthogonal directions $\mathbf{u}_s$ and $\mathbf{w}_s$
$\theta(s,u,t), \phi(s,u,t),$ and $\delta(s,u,t)$	oriented angles $(\mathbf{u}_z, \mathbf{u}_s)$ , $(\mathbf{u}_r, \mathbf{u}_u)$ , and $(\mathbf{w}_s, \mathbf{u}_u)$ , respectively
$\partial_z^k$	partial derivative with respect to $z$ of order $k$
<b>grad</b>	gradient operator
div	divergence operator
$\partial_{\mathbf{w}_s} = \mathbf{w}_s \cdot \mathbf{grad}$	partial derivative in the direction $\mathbf{w}_s$
$\Delta = \nabla^2$	Laplacian operator

tions of the pressure exist are then redefined. Finally, Sec. V extends the 1D model to the case of mobile walls having small admittances. The model is first derived, the compatibility of the geometrical hypothesis with this generalization is detailed, and the particular cases of mobile rigid walls and of visco-thermal boundary layers are investigated. (See Table I.)

## II. PROBLEM STATEMENT

Throughout this paper, the problem considered is linear acoustic propagation in guides that are symmetrical with respect to the longitudinal axis ( $Oz$ ). Only axisymmetric excitations are considered so that the whole problem is axisymmetric.

### A. Basic equations

For adiabatic lossless media, the equation of mass conservation<sup>13</sup>

$$\rho_0 c^2 \operatorname{div}(\mathbf{v}) = -\partial_t p, \quad (1)$$

and the equation of momentum conservation

$$\rho_0 \partial_t \mathbf{v} = -\mathbf{grad}(p), \quad (2)$$

yield the wave equation

$$\left( \Delta - \frac{1}{c^2} \partial_t^2 \right) p = 0, \quad (3)$$

where  $p$  denotes the acoustic pressure,  $\mathbf{v}$  is the particle acoustic velocity,  $\rho_0$  is the density of the air, and  $c$  is the speed of sound in air. The boundary conditions will be specified in the following, for each particular case studied.

Because of the symmetry of the problem,  $p$  and  $\mathbf{v}$  only depend on the longitudinal and the transverse coordinates, noted  $z$  and  $r$ , respectively. For this 2D problem, the spatial operators are reduced to<sup>13</sup>

$$\operatorname{div}(\mathbf{v}) = \partial_z(\mathbf{v} \cdot \mathbf{u}_z) + \frac{\mathbf{v} \cdot \mathbf{u}_r}{r} + \partial_r(\mathbf{v} \cdot \mathbf{u}_r), \quad (4)$$

$$\mathbf{grad}(p) = \partial_z p \mathbf{u}_z + \partial_r p \mathbf{u}_r, \quad (5)$$

and

$$\Delta p = \partial_z^2 p + \frac{1}{r} \partial_r p + \partial_r^2 p, \quad (6)$$

where  $\mathbf{u}_z$  and  $\mathbf{u}_r$  are the normal unit vectors, respectively, associated with the coordinates  $z$  and  $r$ , and “ $\cdot$ ” denotes the scalar product.

### B. Prospective goals and description of the problem

Simulating acoustic propagation in an axisymmetric waveguide requires solving the 2D problem Eq. (3) with Eq. (6) for the boundary conditions on the wall, as well as at the input and the output of the guide. For instance, target applications may require wall conditions such as motionless rigid walls (possibly with visco-thermal boundary layers) for models of wind instruments, or controlled moving and vibrating walls for vocal tract models. The purpose of this paper is to propose a method to derive models of such waveguides, which do not require a resolution in the 2D-inside space, allowing low-cost simulations (e.g., real-time applications). The idea developed in the following consists of reducing the 2D problem to a 1D complexity such as the Webster equation does, making assumptions as weak as possible.

The first step of the method is to separate the geometrical information carried by the time-varying isobaric maps from that of the propagation of the pressure travelling on it. This is done considering a change of coordinates  $(z,r) = (f(s,u,t), g(s,u,t))$  where  $s$  is chosen as an isobar index (Sec. III B), defining  $f$  and  $g$  in an implicit way [Eq. (15)].

Thus,  $z$  and  $r$  become (like the pressure) dependent variables of the partial differential equation which models the wave equation: they describe the isobaric map with respect to the independent variables  $(s,u,t)$ . Writing that  $s$  indexes isobars [Eq. (15)] enables the derivation of the gradient of the pressure [Eq. (19)] and the wave equation [Eq. (20)] for

$(s, u, t)$ . This last equation exactly models the coupling of the propagation of the pressure with the isobaric map geometry, maps for which a necessary condition is straightforwardly deduced [Eq. (24)] and time-invariant specimens are exhibited (Sec. III D).

As the pressure does not depend on  $u$ , having explicit expressions of the coefficients of the wave equation for a given  $u$  suffices to furnish 1D models. Choosing to describe the wall for a constant  $u = w$  leads to an explicit parametrization  $f|_w, g|_w$  of the wall [Eq. (40)]. An additional hypothesis is needed to separate the propagation and the geometrical problems because partial derivatives of  $f$  and  $g$  with respect to  $u$  are involved.

The hypothesis of quasisphericity of isobars near the wall [Eq. (49)] makes the isolation of these problems possible. For lossless and motionless rigid walls, the deduced 1D model [Eq. (51)] can be written for a  $z$  description of the wall [Eq. (54)] or an  $\ell$ -description [Eq. (55)] which leads to a Webster equation,  $\ell$  measuring the arc length of the wall. For more general wall conditions, the 1D model [Eq. (69)] requires that isobars are nearly orthogonal to the wall (Sec. V B) to preserve the linearity of the propagation with respect to the pressure. This is fulfilled for mobile walls in many practical cases and for motionless rigid walls which induce visco-thermal losses, leading to the models in Eq. (78) and Eq. (82), respectively.

### III. DERIVATION OF EXACT EQUATIONS

This section establishes the wave equation in any coordinate system rectifying the isobaric map for axisymmetric problems. The calculations are exact whenever isobaric maps can be locally described by a  $\mathcal{C}^2$ -regular diffeomorphism  $\Phi$ ; that is,  $\Phi$  has an inverse  $\Phi^{-1}$  and both have continuous derivatives up to the second order. Although topological aspects are not discussed here, a necessary geometrical condition is given for the map's admissibility. Before the method is described, the various geometrical quantities involved are precisely defined for an arbitrary change of coordinates. The definitions and the notations of this preliminary part constitute the reference list of the geometrical quantities used in this paper.

#### A. Geometrical definitions

Let  $O$  and  $\mathcal{B}^0 = (\mathbf{u}_z, \mathbf{u}_r)$  be the origin located on the axis of symmetry and the oriented canonical basis of the reference 2D frame  $(O, z, r)$ , respectively. Let  $\Phi$  be an arbitrary regular diffeomorphism defining a spatiotemporal change of coordinates  $(s, u, t) = \Phi(z, r, t)$ , which does not distort time. Then, the functions  $f$  and  $g$  defined by

$$z = f(s, u, t), \quad (7a)$$

$$r = g(s, u, t), \quad (7b)$$

exist and have the same regularity as  $\Phi$ . Coordinates  $s$  and  $u$  are commonly called curvilinear because the variation of one of them does not make the corresponding point describe a straight line in the original space. The associated curves are noted, for each time  $t$ ,

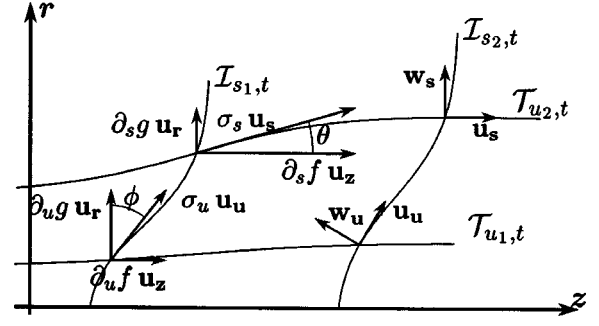


FIG. 1. Definition of the geometrical quantities related to the local basis  $\mathcal{B}_t$ . Note that although all represented vectors and angles coexist at every point located at  $(s, u)$ , various quantities are described for several distinct points to improve the clarity and legibility of the figure.

$\mathcal{T}_{u,t}$  if  $s$  varies and  $u$  remains constant,

$\mathcal{T}_{s,t}$  if  $u$  varies and  $s$  remains constant.

If  $\Phi$  has a  $\mathcal{C}^1$  regularity, a spatial local basis  $\mathcal{B}_t$  for the  $(s, u)$ -coordinate system may be defined for each time  $t$  by the vectors  $\partial_s f \mathbf{u}_z + \partial_s g \mathbf{u}_r$  and  $\partial_u f \mathbf{u}_z + \partial_u g \mathbf{u}_r$ . Then, their respective norms  $\sigma_s$  and  $\sigma_u$ , their associated unit vectors  $\mathbf{u}_s$  and  $\mathbf{u}_u$ , and the characteristic oriented angles  $\theta = (\mathbf{u}_z, \mathbf{u}_s)$  and  $\phi = (\mathbf{u}_r, \mathbf{u}_u)$  are defined. These geometrical quantities represented in Fig. 1 are given by the following expressions:

$$\sigma_s = \sqrt{(\partial_s f)^2 + (\partial_s g)^2}, \quad (8a)$$

$$\sigma_u = \sqrt{(\partial_u f)^2 + (\partial_u g)^2}, \quad (8b)$$

$$\cos \theta = \partial_s f / \sigma_s, \quad (9a)$$

$$\sin \theta = \partial_s g / \sigma_s, \quad (9b)$$

$$\cos \phi = \partial_u g / \sigma_u, \quad (9c)$$

$$\sin \phi = -\partial_u f / \sigma_u, \quad (9d)$$

$$\mathbf{u}_s = \cos \theta \mathbf{u}_z + \sin \theta \mathbf{u}_r, \quad (10a)$$

$$\mathbf{u}_u = -\sin \phi \mathbf{u}_z + \cos \phi \mathbf{u}_r. \quad (10b)$$

For convenience, the vectors  $\mathbf{u}_s$  and  $\mathbf{u}_u$  rotated counterclockwise through the angle  $+\pi/2$  are also introduced, namely,

$$\mathbf{w}_s = -\sin \theta \mathbf{u}_z + \cos \theta \mathbf{u}_r, \quad (11a)$$

$$\mathbf{w}_u = -\cos \phi \mathbf{u}_z - \sin \phi \mathbf{u}_r. \quad (11b)$$

Then, the default of orthogonality of  $\mathcal{B}_t$  can be exhibited by the angular deviation  $\delta = (\mathbf{w}_s, \mathbf{u}_u)$  and more generally by its tangent  $\epsilon$  given by

$$\delta = \phi - \theta, \quad (12a)$$

$$\epsilon = \tan \delta. \quad (12b)$$

Indeed, a local basis  $\mathcal{B}_t$  is orthogonal if and only if  $\epsilon = 0$ . This is also equivalent to  $\mathbf{u}_s \cdot \mathbf{u}_u = 0$  which yields the useful relation

$$\partial_s f \partial_u f + \partial_s g \partial_u g = 0. \quad (13)$$

Finally, the Mach numbers  $\xi_s = (1/c) \mathbf{V} \cdot \mathbf{u}_s$  and  $\xi_u = (1/c) \mathbf{V} \cdot \mathbf{u}_u$  associated with the tangential and the normal components of the velocity  $\mathbf{V}$  of a geometrical point (not that

of the particle) located at  $(s, u)$ , respectively, are introduced. These dynamic quantities are given by

$$\xi_s = \frac{1}{c} [\partial_t f \cos \theta + \partial_t g \sin \theta], \quad (14a)$$

$$\xi_n = \frac{1}{c} [-\partial_t f \sin \theta + \partial_t g \cos \theta]. \quad (14b)$$

Note that a coordinate system compatible with the axial symmetry is such that for all  $u, t$ , there exists a  $u^*$  such that, for all  $s$ ,

$$f(s, u^*, t) = f(s, u, t),$$

$$g(s, u^*, t) = -g(s, u, t).$$

This implies in particular that for each time, there exists  $u_0$  such that  $\mathcal{T}_{u_0, t}$  is the axis of symmetry. Generally, given an axisymmetric map  $\{\mathcal{I}_{s, t}, \mathcal{T}_{u, t}\}$ , a natural choice for its description consists of using  $f$  and  $g$  which have an even and odd  $u$ -parity, respectively.

## B. Rectification of the isobaric map

A change of coordinates  $\Phi$  which rectifies the isobaric map is such that one ordinate indexes isobars while the other is not colinear to the first one to preserve  $\Phi$  as a bijection. Conferring the indexation of isobars to  $s$  signifies that, for each time  $t$ , the curves  $\mathcal{I}_{s, t}$  represent the isobars while the curves  $\mathcal{T}_{u, t}$  are nowhere tangent to  $\mathcal{I}_{s, t}$  (see Fig. 2).

Thus, for any given  $s$ , the pressure does not depend on  $u$ , so the local rectification on a domain  $\Omega$  is obtained for the following condition: there exists a function  $\tilde{p}$ , such that for all  $(s, u, t)$  in  $\Omega$ ,

$$p(f(s, u, t), g(s, u, t), t) = \tilde{p}(s, t). \quad (15)$$

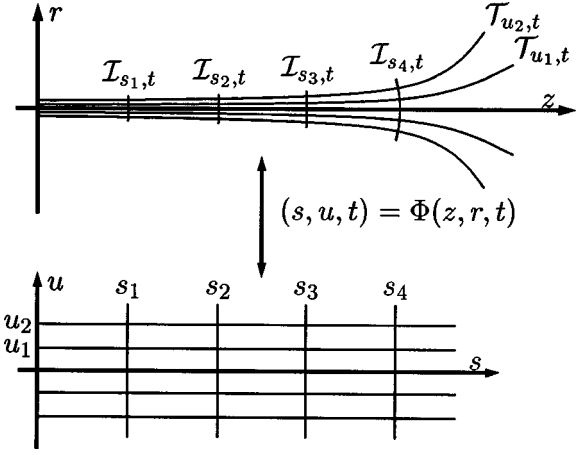


FIG. 2. This figure gives an example of a change of coordinates which rectifies the isobaric maps at a given time  $t$ , and for which  $u$  indexes the field lines. For the coordinate system  $(s, u)$ , the pressure does not vary with  $u$ . In this illustration, the simple topology of isobars ( $\mathcal{I}_{s, t}$ ) makes the definition of the diffeomorphism  $\Phi$  possible over the whole map. When more complex topologies appear (closed curves, singular points, splitting curve, etc.), several changes of coordinates should be considered on local domains. The study of a global resolution for such topologies is not discussed here.

Assuming the  $\mathcal{C}^2$  regularity for  $f$ ,  $g$ , and  $\tilde{p}$ , this implicit relation on  $f$  and  $g$  makes the derivation of the wave equation which governs  $\tilde{p}$  possible on  $\Omega$ . The method consists of expressing the partial derivatives of  $p(z, r, t)$  evaluated in  $(z, r, t) = (f(s, u, t), g(s, u, t), t)$  from the partial derivatives of  $\tilde{p}(s, t)$ , as described below.

Applying the differential operators  $\partial_s$ ,  $\partial_u$ , and  $\partial_t$  on Eq. (15) up to the second order leads to the system

$$\tilde{\mathcal{D}}(s, u, t) = \mathcal{M}(s, u, t) \mathcal{D}(f(s, u, t), g(s, u, t), t). \quad (16)$$

The corresponding explicit formulation is developed in Eq. (17), omitting the variables of evaluation for sake of compactness,

$$\underbrace{\begin{bmatrix} \partial_s \tilde{p} \\ \partial_u \tilde{p} \\ \partial_t \tilde{p} \\ \partial_s^2 \tilde{p} \\ \partial_u^2 \tilde{p} \\ \partial_t^2 \tilde{p} \\ \partial_s \partial_u \tilde{p} \\ \partial_s \partial_t \tilde{p} \\ \partial_u \partial_t \tilde{p} \end{bmatrix}}_{\tilde{\mathcal{D}}} = \underbrace{\begin{bmatrix} \partial_s f & \partial_s g & 0 & 0 & 0 & 0 & 0 & 0 & 0 \\ \partial_u f & \partial_u g & 0 & 0 & 0 & 0 & 0 & 0 & 0 \\ \partial_t f & \partial_t g & 1 & 0 & 0 & 0 & 0 & 0 & 0 \\ \partial_s^2 f & \partial_s^2 g & 0 & (\partial_s f)^2 & (\partial_s g)^2 & 0 & 2\partial_s f \partial_s g & 0 & 0 \\ \partial_u^2 f & \partial_u^2 g & 0 & (\partial_u f)^2 & (\partial_u g)^2 & 0 & 2\partial_u f \partial_u g & 0 & 0 \\ \partial_t^2 f & \partial_t^2 g & 0 & (\partial_t f)^2 & (\partial_t g)^2 & 1 & 2\partial_t f \partial_t g & 2\partial_t f & 2\partial_t g \\ \partial_s \partial_u f & \partial_s \partial_u g & 0 & \partial_s f \partial_u f & \partial_s g \partial_u g & 0 & \partial_s f \partial_u g + \partial_u f \partial_s g & 0 & 0 \\ \partial_s \partial_t f & \partial_s \partial_t g & 0 & \partial_s f \partial_t f & \partial_s g \partial_t g & 0 & \partial_s f \partial_t g + \partial_t f \partial_s g & \partial_s f & \partial_s g \\ \partial_u \partial_t f & \partial_u \partial_t g & 0 & \partial_u f \partial_t f & \partial_u g \partial_t g & 0 & \partial_u f \partial_t g + \partial_t f \partial_u g & \partial_u f & \partial_u g \end{bmatrix}}_{\mathcal{M}} \underbrace{\begin{bmatrix} \partial_z p \\ \partial_r p \\ \partial_t p \\ \partial_z^2 p \\ \partial_r^2 p \\ \partial_t^2 p \\ \partial_z \partial_r p \\ \partial_z \partial_t p \\ \partial_r \partial_t p \end{bmatrix}}_{\mathcal{D}}. \quad (17)$$

Then,  $\mathcal{D}$  is formally obtained from Eq. (16) by computing  $\mathcal{M}^{-1} \tilde{\mathcal{D}}$  and remarking that

$$\tilde{\mathcal{D}}^T = [\partial_s \tilde{p}, 0, \partial_t \tilde{p}, \partial_s^2 \tilde{p}, 0, \partial_t^2 \tilde{p}, 0, \partial_s \partial_t \tilde{p}, 0], \quad (18)$$

since  $\partial_u \tilde{p}(s, t) = 0$ . Expressions expressed explicitly with the

monospace dependent pressure  $\tilde{p}(s, t)$  are straightforwardly deduced for the gradient from Eq. (5) and for the wave equation from Eq. (3) and Eq. (6) evaluated in  $(z, r, t) = (f(s, u, t), g(s, u, t), t)$ . After simplification and using the



notations defined in Sec. III A, these relations become

$$\mathbf{grad}(\tilde{p}) = \frac{\partial_s \tilde{p}}{\sigma_s} [\mathbf{u}_s + \epsilon \mathbf{w}_s] \quad (19)$$

and

$$A_{s,s} \partial_s^2 \tilde{p} + A_s \partial_s \tilde{p} + A_{s,t} \partial_s \partial_t \tilde{p} - \frac{1}{c^2} \partial_t^2 \tilde{p} = 0, \quad (20)$$

where the coefficients given by

$$A_{s,s} = \frac{1 + \epsilon^2 - (\xi_s + \epsilon \xi_n)^2}{\sigma_s^2}, \quad (21a)$$

$$A_s = \frac{\sin \theta + \epsilon \cos \theta}{g \sigma_s} + \frac{1 - \xi_n^2}{\sigma_s^2} \left[ \partial_s (\epsilon^2) + (1 + \epsilon^2) \left( \frac{\sigma_s \partial_u \phi}{\sigma_u \cos \delta} \right. \right. \\ \left. \left. + \epsilon \partial_s \theta - \partial_s \ln \sigma_s \right) \right] - \frac{1}{2} \partial_s \left( \frac{\xi_s^2 + 2 \epsilon \xi_s \xi_n - \xi_n^2}{\sigma_s^2} \right) \quad (21b)$$

$$- \frac{\xi_s \xi_n}{\sigma_s^2} \partial_s \epsilon + \frac{1}{c} \partial_t \left( \frac{\xi_s + \epsilon \xi_n}{\sigma_s} \right) + \frac{\xi_n}{c \sigma_s} \partial_t \epsilon, \quad (21b)$$

$$A_{s,t} = 2 \frac{\xi_s + \epsilon \xi_n}{c \sigma_s}, \quad (21c)$$

are expressions of  $f$  and  $g$  exclusively and depend on  $(s, u, t)$ . Although the tedious calculations are not detailed, note that this process cannot be reduced to writing the Laplacian operator for the change of coordinates  $\Phi$ , as for usual static coordinates. Thus, the Mach numbers  $\xi_s$  and  $\xi_n$  involved in Eqs. (21) are precisely the contribution of the term  $\partial_t^2 p$  in Eq. (3). They are the expression of the dynamic of the isobaric map.

Note that choosing  $u$  such that  $\mathcal{T}_{u,t}$  represent the field lines leads without loss of generality to simpler expressions for which  $\epsilon=0$  because of the orthogonality of  $\mathcal{T}_{s,t}$  and  $\mathcal{T}_{u,t}$  at each point. This concise formulation is exploited in Sec. III D to exhibit static maps, and in Sec. IV to derive a monospace dependent wave equation for motionless rigid walls. However, the study dealing with mobile walls having small admittances presented in Sec. V requires being driven with nonorthogonal coordinates so that Eq. (20) is established in this more general context.

A remarkable property of these equations is that they are not modified by any bijective regular change of variables such that  $s = \alpha(\hat{s}, \hat{t})$ ,  $u = \beta(\hat{s}, \hat{u}, \hat{t})$ , and  $t = \hat{t}$ : taking  $\hat{s}$ ,  $\hat{u}$ ,  $\hat{t}$ ,  $\hat{f}(\hat{s}, \hat{u}, \hat{t}) = f(\alpha(\hat{s}, \hat{t}), \beta(\hat{s}, \hat{u}, \hat{t}), \hat{t})$ ,  $\hat{g}(\hat{s}, \hat{u}, \hat{t}) = g(\alpha(\hat{s}, \hat{t}), \beta(\hat{s}, \hat{u}, \hat{t}), \hat{t})$ , and  $\hat{p}(\hat{s}, \hat{t}) = \tilde{p}(\alpha(\hat{s}, \hat{t}), \hat{t})$ , in place of  $s$ ,  $u$ ,  $t$ ,  $f$ ,  $g$ , and  $\tilde{p}$  keeps the formula identical. Moreover, the axial symmetry is also naturally supported by the isobaric wave equation. Indeed, for  $f$  and  $g$  having an even and odd  $u$ -parity, respectively, applying  $u \rightarrow -u$  in Eq. (20) leaves this equation invariant.

### C. Regular isobaric maps and admissibility

A necessary condition for isobaric maps, which is independent of the pressure, can be deduced from Eq. (20) on  $(f, g)$ . This criterion of admissibility furnishes a property

inherent in the set of regular isobaric maps. It proves in particular that any arbitrary regular map does not always match with a wave propagation phenomenon.

The derivation of this condition relies on the  $u$ -independence of  $\tilde{p}$ . The method consists of applying operators  $\partial_u^k$  in Eq. (20). As the factors represented by  $\mathcal{P} = [\partial_s^2 \tilde{p}, \partial_s \tilde{p}, \partial_s \partial_t \tilde{p}, \partial_t^2 \tilde{p}]^T$ , do not depend on  $u$ , they may be eliminated by making linear combinations of four distinct relations proceeding from four distinct integers  $k$ . In fact, only three of these relations suffice as the proof below describes.

If the  $\mathcal{C}^2$  functions  $f$  and  $g$  have in addition a  $\mathcal{C}^5$ -regularity for the variable  $u$ , the operators  $\partial_u^k$  ( $k=0,1,2,3$ ) applied on Eq. (20) yield the system

$$\mathcal{A}\mathcal{P} = 0, \quad (22)$$

where

$$\mathcal{A} = \begin{bmatrix} A_{s,s} & A_s & A_{s,t} & -\frac{1}{c^2} \\ \partial_u A_{s,s} & \partial_u A_s & \partial_u A_{s,t} & 0 \\ \partial_u^2 A_{s,s} & \partial_u^2 A_s & \partial_u^2 A_{s,t} & 0 \\ \partial_u^3 A_{s,s} & \partial_u^3 A_s & \partial_u^3 A_{s,t} & 0 \end{bmatrix}. \quad (23)$$

For a propagative phenomenon  $\mathcal{P} \neq 0$ ,  $\mathcal{P}$  is then an eigenvector of  $\mathcal{A}$  associated with the eigenvalue 0. This proves that  $\det(\mathcal{A}) = 0$ . By developing the determinant with respect to the last column, a simpler equivalent formulation is obtained for

$$\det \begin{bmatrix} \partial_u A_{s,s} & \partial_u A_s & \partial_u A_{s,t} \\ \partial_u^2 A_{s,s} & \partial_u^2 A_s & \partial_u^2 A_{s,t} \\ \partial_u^3 A_{s,s} & \partial_u^3 A_s & \partial_u^3 A_{s,t} \end{bmatrix} = 0. \quad (24)$$

This necessary condition only involves the equations derived for  $k=1,2,3$ . Equation (24) closes the proof since  $A_{s,s}$ ,  $A_s$ , and  $A_{s,t}$  depend on  $f$  and  $g$  only, and thus, on the dynamic geometry.

The criterion Eq. (24) can be straightforwardly computed for any given maps to check their admissibility. Except for a few trivial dynamic and geometrical starting conditions, an analytic derivation of admissible maps from this criterion becomes very tricky.

### D. Static isobaric maps

This section presents an investigation into the restricted case of static maps on which propagative waves may travel. In order to exhibit the physical propagative solutions only, the pressure is assumed to be such that the functions  $\partial_s^2 \tilde{p}$ ,  $\partial_s \tilde{p}$ , and  $\partial_t^2 \tilde{p}$  are nonzero and real. The investigation is run directly from the isobaric wave equation rather than the admissibility criterion which only gives a necessary condition.

A static map may be described by time-independent functions  $f(s, u)$  and  $g(s, u)$ . Choosing  $\mathcal{T}_u$  as the field lines yields the constraint  $\epsilon=0$ . Thus, the solution map is represented without loss of generality by  $(f, g)$  satisfying Eq. (13) and

$$\partial_s^2 \tilde{p} + \partial_s \mathcal{L} \partial_s \tilde{p} - \frac{\sigma_s^2}{c^2} \partial_t^2 \tilde{p} = 0, \quad (25)$$

calculated from Eq. (20) multiplied by  $\sigma_s^2$ .  $\mathcal{L}$  is given by

$$\mathcal{L} = \ln \left| g \frac{\sigma_u}{\sigma_s} \right|, \quad (26)$$

remarking that Eq. (13) implies  $\partial_u \phi / \cos^3 \delta = \partial_u \theta = \partial_s \sigma_u / \sigma_s$ . Then, two cases are examined separately:  $\sigma_s$  depends on  $s$  only, or on  $(s, u)$ .

### 1. $\sigma_s$ does not depend on $u$

In this case,  $\partial_s \mathcal{L}$  does not depend on  $u$  either [see Eq. (25)]. Parallel planes orthogonal to  $(Oz)$  and coaxial cylinders are obtained for  $\partial_s g = 0$  and  $\partial_u g = 0$ , respectively. Except for these pathological cases, Eq. (13) ensures that  $\partial_s f$ ,  $\partial_u f$ ,  $\partial_s g$ , and  $\partial_u g$  are nonzero.

Then, Eq. (13) makes the elimination of  $\partial_s f$  possible in  $\partial_u(\sigma_s^2) = 0$  calculated from the definition Eq. (8a). The result  $\partial_s \ln |\partial_u g| = \partial_s \ln |\partial_u f|$  equivalent to  $\partial_s \ln |\tan \phi| = 0$  [see Eq. (9c) and Eq. (9d)] proves that  $\phi$  depends only on  $u$ . As  $\epsilon = \tan(\phi - \theta)$  is zero,  $\theta$  is an exclusive function of  $u$  as well. Equations (9a) and (9b) show that

$$f(s, u) = R(s) \cos \theta(u) + F(u), \quad (27a)$$

$$g(s, u) = R(s) \sin \theta(u) + G(u), \quad (27b)$$

where  $R' = \sigma_s$ , and  $F$  and  $G$  are arbitrary.

Now, from Eq. (9c),  $\sigma_u = \partial_u g / \cos \phi$  so that  $\partial_s \partial_u \mathcal{L} = 0$  can be written  $\partial_u \partial_s \ln |g \partial_u g| = 0$  which, with Eq. (27b), leads to

$$G(u) = R_0 \sin \theta(u),$$

$R_0$  being an arbitrary constant. Finally, the calculation of Eq. (13) using Eqs. (27) with this function  $G$  yields

$$F(u) = R_0 \cos \theta(u) + F_0,$$

where  $F_0$  is arbitrary. The corresponding isobars are concentric spheres. This conclusion completes the proof that parallel planes, coaxial cylinders, and concentric spheres are the only static isobaric maps for which  $\sigma_s$  does not depend on  $u$ .

### 2. $\sigma_s$ depends on $u$

In this case,  $\partial_s \mathcal{L}$  also depends on  $u$ . Applying  $\partial_u$  to Eq. (25) leads to

$$\partial_u \partial_s \mathcal{L} \partial_s \tilde{p} - \frac{\partial_u(\sigma_s^2)}{c^2} \partial_t^2 \tilde{p} = 0.$$

Since  $\partial_u \sigma_s$  and  $\partial_s \tilde{p}$  are assumed nonzero, this relation proves that  $\partial_t^2 \tilde{p} / \partial_s \tilde{p}$  does not depend on  $t$ . Then, Eq. (25) proves that  $\partial_s^2 \tilde{p} / \partial_s \tilde{p} = \partial_s \ln |\tilde{p}|$  does not depend on  $t$  either, so that a general solution is  $\tilde{p}(s, t) = A(s)b(t) + C(t)$  where  $A$ ,  $b$ , and  $C$  are real functions. Writing Eq. (25) for this solution and applying the operator  $X \mapsto \partial_t(X/b(t))$  on it show that both  $c^{-2}b''(t)/b(t) = -k_0^2$  and  $C''(t)/b(t) = C_0$  are real constants so that  $C(t) = C_0 b(t) + C_1 t + C_2$  with  $(C_1, C_2) \in \mathbb{R}^2$ . Defining  $a(s) = A(s) + C_0$ , this proves that the general solution is

$$\tilde{p}(s, t) = a(s)b(t) + C_1 t + C_2,$$

with

$$b(t) = B_1 e^{ik_0 ct} + B_2 e^{-ik_0 ct},$$

where  $B_1, B_2$  are complex arbitrary constants such that  $b(t)$  is real. Although it does not affect the following, note that physical cases require that  $C_1 = C_2 = 0$  since  $\tilde{p}$  is the acoustic pressure.

Using Eq. (26), Eq. (25) is then reduced to

$$\partial_s \ln |a| \partial_s \ln \left| \frac{a'}{\sigma_s} g \sigma_u \right| + (k_0 \sigma_s)^2 = 0.$$

Moreover, if the spatial dependence  $a$  for the wave number  $k_0$  is locally bijective, posing  $\hat{s} = a(s)$ , and then defining  $\hat{f}(\hat{s}, u, t) = f(s, u, t)$  and  $\hat{g}(\hat{s}, u, t) = g(s, u, t)$  yields

$$\partial_{\hat{s}} \ln \left| \frac{\hat{g} \hat{\sigma}_s}{\hat{\sigma}_u} \right| + (k_0 \sigma_s)^2 \hat{s} = 0.$$

This equation shows that every static map such that  $\sigma_s$  depends on  $u$  is associated with a time dependency corresponding to a pure frequency ( $k_0$  real) or a pure exponential ( $k_0$  imaginary). More precisely, once given the geometry of the wall parameterized with  $s, u$  and expressing the boundary conditions, this last equation and Eq. (13) give the isobaric map associated with the wave number  $k_0$ .

### 3. Conclusion: Theorem

- (i) Parallel planes, coaxial cylinders, and concentric spheres are the only static axisymmetric isobaric geometries on which non-necessarily sinusoidal or exponential waves can propagate.
- (ii) Other static geometries are associated with a wave number  $k_0 \in \mathbb{R}^+ \cup i\mathbb{R}^+$  which characterizes the geometric invariant given by

$$\frac{\partial_{\hat{s}} \ln \left| \frac{\hat{g} \hat{\sigma}_s}{\hat{\sigma}_u} \right|}{\hat{s} \hat{\sigma}_s^2} = -k_0^2, \quad (28)$$

where  $\hat{s}$  denotes the level of the spatial dependence of the pressure and  $u$  is orthogonal to  $\hat{s}$ .

The first part of this theorem (i) corroborates the result of Putland<sup>8</sup> who exhibited parallel planes, coaxial cylinders, and concentric spheres as the only maps making the separation of variables possible. Nevertheless, other maps exist even if they are associated with particular waveforms (sinusoidal or exponential). This last case would correspond to having the Wronskian defined by Putland being zero, a case that he discarded [see Eqs. (19) and (20) in his paper].

### 4. Example of a static map

As only a few of them can be performed analytically, knowing that all the modal static maps satisfy Eq. (28) can be very useful. However, it is interesting to illustrate this second part of the theorem through an example for which the spatial dependence takes an analytical expression.

The example, detailed below, concerns the field of pressure inside a paraboloid of revolution. Using the separation principle of the Helmholtz equation for the orthogonal parabolic coordinates<sup>14</sup>  $(\mu, \nu) \in \mathbb{R}^+ \times \mathbb{R}$  defined by

$$z = (1/2)(\mu^2 - \nu^2), \quad (29a)$$

$$r = \mu \nu, \quad (29b)$$

a particular solution of the wave equation is proven to be

$$P_0 J_0\left(\frac{k_0}{2} \mu^2\right) J_0\left(\frac{k_0}{2} \nu^2\right) \cos(c k_0(t - t_0)), \quad (30)$$

where  $P_0$  and  $t_0$  are arbitrary real constants, and  $J_0$  is the 0th order Bessel function of the first kind. This solution can be checked straightforwardly from Eq. (3) and Eq. (6) using the reciprocal change of coordinates  $(1/2)\mu = \sqrt{z + \sqrt{z^2 + r^2}}$  and  $\nu = r/\mu$ , and recalling that

$$J_0''(X) = \frac{J_0'(X)}{X} - J_0(X). \quad (31)$$

Now, for the wave number  $k_0$ , the isobaric map is such that

$$\hat{s} = J_0\left(\frac{k_0}{2} \mu(\hat{s}, u)^2\right) J_0\left(\frac{k_0}{2} \nu(\hat{s}, u)^2\right), \quad (32)$$

where  $\hat{s}$  defines the level of the spatial dependence of the pressure. It is represented in Fig. 3.

As expected, the second part (ii) of the theorem is satisfied. However, because the definition of the  $\hat{s}$ -level curves is implicit [Eq. (32)], the proof is not straightforward as detailed below.

From  $\hat{f}(\hat{s}, u) = (1/2)(\mu(\hat{s}, u)^2 - \nu(\hat{s}, u)^2)$  and  $\hat{g}(\hat{s}, u) = \mu(\hat{s}, u)\nu(\hat{s}, u)$ , it follows that  $\hat{\sigma}_s^2 = (\mu^2 + \nu^2)[(\partial_s \mu)^2 + (\partial_s \nu)^2]$ ,  $\hat{\sigma}_u^2 = (\mu^2 + \nu^2)[(\partial_u \mu)^2 + (\partial_u \nu)^2]$ , and that the orthogonality Eq. (13) of  $(\hat{s}, u)$  is also given by

$$\partial_s \mu \partial_u \mu + \partial_s \nu \partial_u \nu = 0. \quad (33)$$

These equations yield  $\partial_s \hat{\mathcal{L}} = \partial_s \ln|\mu \nu \partial_u \nu / \partial_s \mu|$ .

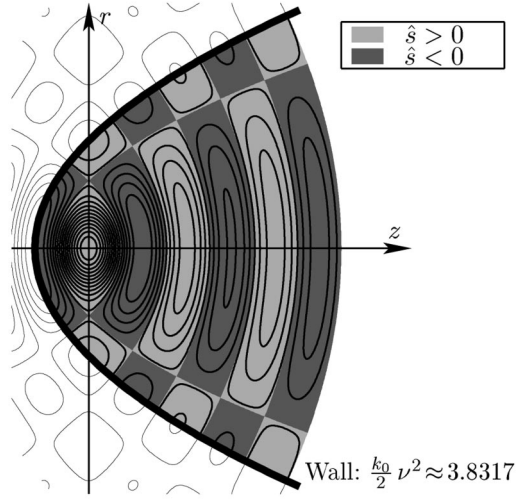


FIG. 3. The  $\hat{s}$ -level curves given by Eq. (32) define the static isobaric map for an oscillating mode of wave number  $k_0$ . This map can be defined over the whole space, but it also corresponds to that inside paraboloids described by a constant  $\nu$ -coordinate, such that  $J_0'[(k_0/2)\nu^2] = 0$ . Indeed, the boundary condition of rigid walls is fulfilled on such paraboloids (the gradient of the pressure has no component orthogonal to the wall). This figure presents the wall associated with the first zero of  $J_0'$ , namely,  $(k_0/2)\nu^2 \approx 3.8317$ .

Applying  $\partial_s$  and  $\partial_u$  to Eq. (32) leads to

$$\partial_s \mu = \frac{1 - k_0 \nu J_0'\left(\frac{k_0}{2} \nu^2\right) J_0\left(\frac{k_0}{2} \mu^2\right) \partial_s \nu}{k_0 \mu J_0'\left(\frac{k_0}{2} \mu^2\right) J_0\left(\frac{k_0}{2} \nu^2\right)}, \quad (34a)$$

$$\partial_u \mu = - \frac{\nu J_0'\left(\frac{k_0}{2} \nu^2\right) J_0\left(\frac{k_0}{2} \mu^2\right)}{\mu J_0'\left(\frac{k_0}{2} \mu^2\right) J_0\left(\frac{k_0}{2} \nu^2\right)} \partial_u \nu. \quad (34b)$$

Substituting  $\partial_s \mu$  and  $\partial_u \mu$  in Eq. (33) yields (for  $\partial_u \nu \neq 0$ )

$$\partial_s \nu = \frac{\nu J_0'\left(\frac{k_0}{2} \nu^2\right) J_0\left(\frac{k_0}{2} \mu^2\right)}{k_0 \left[ \left( \mu J_0'\left(\frac{k_0}{2} \mu^2\right) J_0\left(\frac{k_0}{2} \nu^2\right) \right)^2 + \left( \nu J_0'\left(\frac{k_0}{2} \nu^2\right) J_0\left(\frac{k_0}{2} \mu^2\right) \right)^2 \right]}, \quad (35)$$

and then from Eq. (34a)

$$\partial_s \mu = \frac{\mu J_0'\left(\frac{k_0}{2} \mu^2\right) J_0\left(\frac{k_0}{2} \nu^2\right)}{k_0 \left[ \left( \mu J_0'\left(\frac{k_0}{2} \mu^2\right) J_0\left(\frac{k_0}{2} \nu^2\right) \right)^2 + \left( \nu J_0'\left(\frac{k_0}{2} \nu^2\right) J_0\left(\frac{k_0}{2} \mu^2\right) \right)^2 \right]}. \quad (36)$$

These last equations give expressions of  $\partial_s \mu$  and  $\partial_s \nu$  which do not involve derivatives of  $\mu$  and  $\nu$ . They specifically make the computation of  $\partial_s \hat{\mathcal{L}}$  with this same property possible, overcoming the difficulty due to the implicit definition for the proof. The expressions of  $\partial_s \ln|\mu|$  and  $\partial_s \ln|\nu|$  are straightforward. That of  $\partial_s \ln|\partial_u \nu|$  is computed applying  $\partial_u$  to Eq. (35), substituting occurrences of  $\partial_u \mu$  by  $\partial_u \nu$  according to Eq. (34b), and dividing by the common factor  $\partial_u \nu$ . That of  $\partial_s \ln|\partial_s \mu|$  is computed applying  $\partial_s$  to Eq. (36), dividing by  $\partial_s \mu$ , and substituting occurrences of  $\partial_s \mu$  and  $\partial_s \nu$  according to Eq. (36) and Eq. (35). The two first terms involve  $\mu$ ,  $\nu$ ,  $J_0$ , and  $J_0'$ . The two last also involve  $J_0''$ .

On the one hand, the sum of these terms yields

$$\partial_s \hat{\mathcal{L}} = - \frac{(\mu^2 + \nu^2) J_0 \left( \frac{k_0}{2} \mu^2 \right) J_0 \left( \frac{k_0}{2} \nu^2 \right)}{\left( \mu J_0' \left( \frac{k_0}{2} \mu^2 \right) J_0 \left( \frac{k_0}{2} \nu^2 \right) \right)^2 + \left( \nu J_0' \left( \frac{k_0}{2} \nu^2 \right) J_0 \left( \frac{k_0}{2} \mu^2 \right) \right)^2}, \quad (37)$$

after the substitution of  $J_0''$  according to Eq. (31). On the other hand, computing  $\hat{\sigma}_s^2$  from Eq. (36) and Eq. (35), and using Eq. (32) to compute  $\hat{s}$ , the computation of  $-k_0^2 \hat{s} \hat{\sigma}_s^2$  is straightforward. It exactly yields the right-hand side of Eq. (37), proving Eq. (28).

#### IV. MONO-SPACE-DEPENDENT WAVE EQUATION FOR LOSSLESS AND MOTIONLESS RIGID WALLS

A rigorous derivation of a mono-space model of a waveguide proves to be unworkable for arbitrary geometries. Even if the exact equation (20) governs a mono-space-dependent pressure, expressing  $A_{s,s}$ ,  $A_s$ , and  $A_{s,t}$  from the shape of the waveguide does not succeed in such a 1D model, as described below.

##### A. Problem posed by the derivation of a 1D model

Let  $\Phi$  now be a particular local change of coordinates such that the wall noted  $\mathcal{W}_t$  is simply described for a fixed  $u$  noted  $w$  so that

$$\mathcal{T}_{w,t} = \mathcal{W}_t. \quad (38)$$

This can be achieved if  $\mathcal{W}_t$  is not tangent to isobars, which is discussed below. Adopting the notation

$$q|_w(s,t) = q(s,w,t), \quad (39)$$

to indicate that a quantity  $q(s,u,t)$  is evaluated on the wall  $\mathcal{W}_t$ , the profile of  $\mathcal{W}_t$  is parametrized by

$$z = f|_w(s,t), \quad (40a)$$

$$r = g|_w(s,t). \quad (40b)$$

Then, deriving a 1D model could consist of evaluating the coefficients  $A_{s,s}$ ,  $A_s$ , and  $A_{s,t}$  on  $\mathcal{W}_t$ , namely imposing  $u = w$ , and then, expressing them from the known parametrization  $(f|_w, g|_w)$ . Unfortunately, this cannot be achieved in general. Nevertheless, executing this process reveals the difficulty and, simultaneously, the reason why decoupling the waveform resolution from that of the geometry of isobars is impossible.

This section exhibits the problem for walls assumed ideally rigid, lossless, and motionless:  $\mathcal{T}_{w,t} = \mathcal{W}_t = \mathcal{W}$  so that  $f|_w$  and  $g|_w$  can be chosen time independent and  $\xi_s|_w = \xi_n|_w = 0$  [see Eq. (14)]. In this case, the corresponding boundary condition is that the particle velocity  $\mathbf{v}$ , and so from Eq. (2), the gradient of the pressure  $\mathbf{grad}(p)$ , have no component normal to the wall. For locally nondegenerate cases [ $\mathbf{grad}(p) \neq 0$ ], isobars are necessarily orthogonal to the wall  $\mathcal{W}$ . Considering a domain  $\Omega$  on which this condition is satisfied, this proves that  $\mathcal{W}$  belongs to the field lines so that  $\epsilon|_w = 0$  [see Eq. (12b)]. Note that if the gradient is zero on a set of isolated points, local solutions of the same

1D model can be concatenated to form a maximal solution under the  $\mathcal{C}^2$  regularity assumption. If this set has a nonzero measure, the pressure computed from a mono-space partial differential equation of finite order is necessarily locally constant for both the time and the space variables. On this set, the partial derivatives of the pressure are zero and will make the 1D linear model locally trivial ( $0=0$ ), independently of the involved coefficients. Practically, these properties make it possible to proceed considering only the case  $\epsilon|_w = 0$ , without loss of generality.

Now,  $\epsilon|_w = 0$  and  $\xi_s|_w = \xi_n|_w = 0$  yields, for  $u = w$ , the simplified coefficients  $A_{s,s} = 1/\sigma_s^2$ ,  $A_{s,t} = 0$ , and using Eq. (9b),  $A_s = \partial_s \ln(g/\sigma_s)/\sigma_s^2 + \partial_u \phi/(\sigma_s \sigma_u \cos \delta)$ .

Since  $f|_w$  and  $g|_w$  can be differentiated with respect to  $s$ , then  $\sigma_s$  and  $\partial_s \ln(g/\sigma_s)$  can be evaluated for  $u = w$  using Eq. (8a). On the other hand,  $f|_w$  and  $g|_w$  do not give any information about  $\partial_u f|_w$  and  $\partial_u g|_w$ , and the local orthogonality ( $\epsilon|_w = 0$ ) only yields  $|\cos \delta|_w = 1$ . Thus, starting with  $f|_w$ ,  $g|_w$ , and the relation  $\epsilon|_w = 0$ , one cannot evaluate  $\partial_u \phi/(\sigma_u \cos \delta)$ .

To cope with this difficulty, a local geometrical hypothesis is presented, which gives a natural extension of the exact models of propagation in tubes and cones, and agrees with the isobars mobility.

##### B. Geometrical hypothesis

Let  $M(s)$  be a point of  $\mathcal{W}$  indexed by  $s$ . Let  $\mathcal{S}_s$  be the sphere tangent to  $\mathcal{I}_{s,t}$  at  $M(s)$  and centered at  $O_s \in (Oz)$  (see Fig. 4). Then, the z-ordinate  $z_{O_s}(s)$  of  $O_s$ , the radius

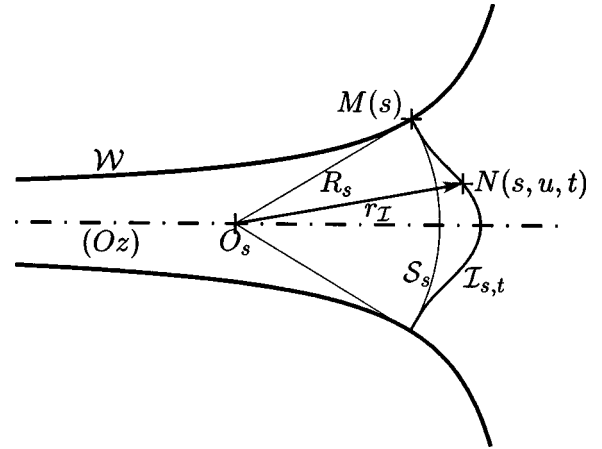


FIG. 4.  $O_s(s) \in (Oz)$  and  $R_s(s)$  are the center and the radius of the sphere  $\mathcal{S}_s$  tangent to  $\mathcal{I}_{s,t}$  at  $M(s) \in \mathcal{W}$ .  $r_I(s, u, t)$  is the distance between  $O_s$  and the point  $N \in \mathcal{I}_{s,t}$  located at  $(s, u, t)$ . It is assumed that  $\mathcal{I}_{s,t}$  and  $\mathcal{S}_s$  are close at the second order at  $M(s)$ . Namely, for each  $(s, t)$ ,  $u \mapsto r_I(s, u, t)$  is approximated by the constant  $R(s)$  at the second order for  $u$  in the vicinity of  $w$ .



$R_s(s)$  of the sphere  $\mathcal{S}_s$ , and for any point  $N(s, u, t)$ , the distance  $r_{\mathcal{I}}(s, u, t)$  between  $O_s$  and  $N$  are defined.

By definition, the radius  $\mathbf{O}_s\mathbf{M}$  is orthogonal to the sphere  $\mathcal{S}_s$  and so to  $\mathbf{u}_u$  at  $M(s)$ . Writing that the scalar product of  $\mathbf{O}_s\mathbf{M}$  and  $\mathbf{u}_u$  is zero,  $z_{O_s}(s)$  is proven to be such that

$$g|_w = \tan \phi|_w (f|_w - z_{O_s}). \quad (41)$$

The positive radii  $R_s(s)$  and  $r_{\mathcal{I}}(s, u, t)$  are given by

$$R_s^2 = \frac{g^2}{\sin^2 \theta} \Big|_w = \frac{g^2}{\sin^2 \phi} \Big|_w, \quad (42a)$$

$$r_{\mathcal{I}}^2 = g^2 + (f - z_{O_s})^2. \quad (42b)$$

The relative divergence  $\varsigma(s, u, t)$  is then introduced by

$$\varsigma = \frac{r_{\mathcal{I}}}{R_s} - 1. \quad (43)$$

$\varsigma$  may be interpreted as an indicator of the deformation engendering  $\mathcal{I}_{s,t}$  from  $\mathcal{S}_s$ . Note that if the wall  $\mathcal{W}$  is locally parallel to  $(Oz)$ ,  $\varsigma$  may keep a meaning by continuation, although  $R_s$  becomes infinite. In particular, the study below proves that  $\varsigma|_w$  is zero at the first order at least.

By definition,  $r_{\mathcal{I}}(s, w, t) = R_s(s)$  so that

$$\varsigma|_w = 0. \quad (44)$$

Now,  $\partial_u \varsigma = \partial_u (r_{\mathcal{I}}^2) / (2r_{\mathcal{I}} R_s)$ . From Eq. (42b), Eq. (9c), and Eq. (9d),

$$\frac{1}{2} \partial_u (r_{\mathcal{I}}^2) = \sigma_u [g \cos \phi - (f - z_{O_s})]. \quad (45)$$

The definition of  $z_{O_s}$  shows that Eq. (45) is zero for  $u = w$  so that

$$(\partial_u \varsigma)|_w = 0. \quad (46)$$

Note that, in fact, this last equation is related to the tangency of  $\mathcal{S}_s$  and  $\mathcal{I}_{s,t}$  at  $M(s)$ . Finally,

$$\partial_u^2 \varsigma = \frac{\partial_u^2 (r_{\mathcal{I}}^2)}{2r_{\mathcal{I}} R_s} - \frac{(\partial_u (r_{\mathcal{I}}^2))^2}{2r_{\mathcal{I}}^2 R_s},$$

so that the second term is zero in  $u = w$  [see Eq. (45)], and

$$\begin{aligned} \frac{1}{2} \partial_u^2 (r_{\mathcal{I}}^2) &= \partial_u \sigma_u [\cos \phi - (f - z_{O_s}) \sin \phi] + \sigma_u^2 \\ &\quad - \sigma_u \partial_u \phi [g \sin \phi + (f - z_{O_s}) \cos \phi], \end{aligned} \quad (47)$$

for which the first term is zero in  $u = w$ . Then,  $(\partial_u^2 \varsigma)|_w$  is given by

$$(\partial_u^2 \varsigma)|_w = \left[ \frac{\sigma_u}{R_s^2} \left( \sigma_u - \frac{g \partial_u \phi}{\sin \phi} \right) \right] \Big|_w. \quad (48)$$

The geometrical hypothesis proposed in this section consists of assuming that near the wall  $\mathcal{W}$ , isobars  $\mathcal{I}_{s,t}$  deviate from  $\mathcal{S}_s$  “slower than a parabola,” namely,

$$(\partial_u^2 \varsigma)|_w = 0. \quad (49)$$

As  $\sigma_u / R_s^2 \neq 0$ , this hypothesis yields

$$\frac{\partial_u \phi}{\sigma_u} \Big|_{s,w,t} = \frac{\sin \phi}{g} \Big|_{s,w,t}, \quad (50)$$

which will make  $A_s|_w$ , and so Eq. (20) for  $u = w$ , possibly be expressed explicitly with  $f|_w$  and  $g|_w$ . Indeed, the right-hand side of Eq. (50) is known from the shape of  $\mathcal{W}$ .

### C. Mono-space wave equation

As  $\epsilon|_w = 0$ ,  $\sin \phi / \cos \delta = \sin \theta = \partial_s g / \sigma_s$  for  $u = w$ . The geometrical hypothesis and this last equation make the evaluation of  $A_s|_w$  possible. Finally, recalling that  $\xi_s|_w = \xi_n|_w = 0$ , this leads to the significantly simplified equation

$$A_{s,s}|_w \partial_s^2 \tilde{p} + A_s|_w \partial_s \tilde{p} - \frac{1}{c^2} \partial_t^2 \tilde{p} = 0, \quad (51)$$

where  $A_{s,s}|_w$  and  $A_s|_w$  are given by

$$A_{s,s}|_w = \frac{1}{\sigma_s^2} \Big|_w, \quad (52a)$$

$$A_s|_w = \frac{2 \partial_s \ln g}{\sigma_s^2} \Big|_w. \quad (52b)$$

Furthermore, because  $\epsilon|_w = 0$ , Eq. (19) leads to

$$\mathbf{grad}(\tilde{p}) = \frac{\partial_s \tilde{p}}{\sigma_s} \mathbf{u}_s, \quad (53)$$

on  $\mathcal{W}$ .

The obtained 1D model is available for any choice made for  $s$ , all the deduced models being equivalent. This model is now established for two specific and natural parametrizations. The first one consists of choosing  $s = z$  so that  $g|_w(s) = R(s)$  represents the radius  $R(z)$  of the section of the waveguide located by the  $z$ -ordinate  $z = f|_w(s) = s$ . In this case,  $\sigma_s(z, w, t) = \sqrt{1 + R'(z)^2}$  leading to

$$\partial_z^2 \tilde{p}(z, t) + 2 \frac{R'(z)}{R(z)} \partial_z \tilde{p}(z, t) - \frac{1 + R'(z)^2}{c^2} \partial_t^2 \tilde{p}(z, t) = 0. \quad (54)$$

Note that this equation does not model the propagation of the lowest mode since it differs from that established by Pagneux<sup>10</sup> [Eq. (45)] when higher-order modes are ignored. The second choice is to take  $s = \ell$  where  $\ell$  measures the arc length of the wall  $\mathcal{W}$  so that  $\sigma_s|_w$  simplifies into the constant 1. Noting  $\mathcal{R}(\ell)$  the radius of the section of the waveguide located by  $\ell$ , the obtained wave equation is that of Webster:

$$\partial_\ell^2 \tilde{p}(\ell, t) + 2 \frac{\mathcal{R}'(\ell)}{\mathcal{R}(\ell)} \partial_\ell \tilde{p}(\ell, t) - \frac{1}{c^2} \partial_t^2 \tilde{p}(\ell, t) = 0. \quad (55)$$

Note that if  $\ell = z = 0$  locates a referent point  $M_0 \in \mathcal{W}$ , the bijective relation between  $\ell$  and  $z$  is given by

$$\ell = L(z) = \int_0^z \sqrt{1 + R'(z)^2} dz. \quad (56)$$

The radius  $\mathcal{R}(\ell)$  is straightforwardly deduced from  $R(z)$  (at least numerically) through the computation of  $L(z)$  since

$$\mathcal{R}(\ell) = R(L^{-1}(\ell)). \quad (57)$$

This last choice makes it possible to attribute all the known properties of the Webster equation to the general model Eq. (51), such as the conservation of acoustic energy, or the existence of analytical solutions for particular profiles. For this reason, Eq. (55) is used in the following rather than Eq. (51) or Eq. (54).

## D. Observations and discussion

As a first result, the hypothesis of quasisphericity Eq. (50) makes the arc length  $\ell$  appear as the natural longitudinal ordinate for the 1D model. This exactly coincides with the ordinate for which Putland establishes the Webster equation. However, the coefficients ahead of  $\partial_\ell \tilde{p}$  are distinct for both models. That of Putland is  $\partial_\ell S(\ell, t)/S(\ell, t)$  where  $S$  denotes the unknown area of the isobaric (or the “ $\ell$ -iso”) surfaces<sup>8</sup> versus  $2\mathcal{R}'/\mathcal{R}$  for Eq. (55) which is known and time-invariant. Considering  $2\mathcal{R}'/\mathcal{R}$  as a ratio  $S'(\ell)/S(\ell)$ , where  $S$  would represent the plane section of the waveguide drawn for  $\ell$  but not  $z$ , yields a similar formulation but remains physically distinct.

Moreover, this model holds various notable properties. First of all, it gives exact results for both straight and conical pipes. Thus, for a straight pipe defined by  $R(z) = R_0$ , and a conical pipe defined by  $R(z) = z \tan \theta_0$  or  $\mathcal{R}(\ell) = \ell \sin \theta_0$  [see Eq. (56)] with  $\theta_0 \in ]0, \pi/2[$ , the 1D model leads to

$$\partial_z^2 \tilde{p}(z, t) - \frac{1}{c^2} \partial_t^2 \tilde{p}(z, t) = 0, \quad (58a)$$

$$\partial_\ell^2 \tilde{p}(\ell, t) + \frac{2}{\ell} \partial_\ell \tilde{p}(\ell, t) - \frac{1}{c^2} \partial_t^2 \tilde{p}(\ell, t) = 0, \quad (58b)$$

respectively. As expected, Eq. (58a) and Eq. (58b) yield the exact models for plane waves and spherical waves.

Compared to the Webster equations established assuming plane, spherical, or oblate spheroidal wavefronts, appreciable improvements of the presented model may be highlighted. Not only is the orthogonality between isobars and the wall respected, but the unavoidable mobility of isobars (see Sec. III D) as well. As a matter of fact, this is a consequence of the locality as well as the minimal order of the hypothesis which only requires  $\partial_u^2 s|_w = 0$  while  $s|_w$  and  $\partial_u s|_w$  are both naturally zero.

Unfortunately, most of the limitations known for the Webster equation remain. The validity of the geometrical hypothesis is restricted to a low frequency range (no transverse mode, e.g., Fig. 3) and smooth geometries so that high mode coupling will not occur.<sup>10</sup> Walls must have a small curvature as well as isobars.

In particular, the model makes the control of the geometry of isobars possible neither at the input nor at the output of the pipe: spheres appear as the best appropriate shapes for the quasisphericity hypothesis. Rigorously, these input–output geometries should be exhibited by solving Eq. (20) for  $(f, g)$  and knowing  $(f|_w, g|_w)$ , once the pressure  $\tilde{p}(s, t)$  has been computed for the 1D model and the 1D boundary conditions. Note that, practically, the geometrical resolution

could be driven with numerical methods and for the simplifying assumption  $\epsilon = 0$ , leading to a description of the isobaric maps by time-varying orthogonal coordinate systems. But since 1D models are generally not exact, the pressure established for any of them should be linked to “aberrant maps” (unsolvable or not axisymmetric). The prospect of deriving a 1D model from Eq. (20) for new more relaxed geometrical hypotheses and making control possible on the boundary isobars will be discussed in the conclusion.

## E. Particular profiles associated with analytical waves

Analytical solutions of the Webster equation are known for particular shapes defined by ( $R_0 > 0$ )

- (i)  $\mathcal{R}(\ell) = R_0 \exp(\alpha \ell)$  (exponential),
- (ii)  $\mathcal{R}(\ell) = R_0 \cosh(\alpha \ell)$  (catenoidal),
- (iii)  $\mathcal{R}(\ell) = R_0 \sin(\alpha \ell)$  (sinusoidal),
- (iv)  $\mathcal{R}(\ell) = R_0 \ell^\alpha$  (Bessel).

This section is dedicated to determining the physical profiles  $R(z)$  corresponding to these four cases.

### 1. Analytical solutions

Noting  $\psi(\ell, \omega)$  the Fourier transform of  $\mathcal{R}(\ell) \tilde{p}(\ell, t)$  where  $\omega$  denotes the angular frequency, the wave equation corresponding to the cases (i–iii) is obtained for

$$\partial_\ell^2 \psi(\ell, \omega) - \left( Y - \frac{\omega^2}{c^2} \right) \psi(\ell, \omega) = 0, \quad (59)$$

where  $Y = \mathcal{R}''(\ell)/\mathcal{R}(\ell)$  is constant. The solutions in the Fourier domain are then

$$\psi(\ell, \omega) = \psi_0(\omega) e^{r(\omega)\ell} + \psi_1(\omega) e^{-r(\omega)\ell}, \quad (60)$$

where  $r(\omega)$  is a square root of  $Y - (\omega/c)^2$  and  $\psi_0, \psi_1$  are arbitrary. When  $Y > 0$ , a cutoff pulsation  $\omega_c = c\sqrt{Y}$  may be defined:  $r(\omega)$  is imaginary and the corresponding wave is propagative only for  $\omega \geq \omega_c$ . Note that although this equation is usually written in this form, Berners<sup>15</sup> has shown that the travelling modes which constitute the Fourier basis set do not furnish a complete set for convex profiles ( $Y < 0$ ). In this case, the equation Eq. (59) must be considered in the Laplace domain rather than that of Fourier. Indeed, he has shown that the set of eigenfunctions may include some so-called “trapped modes.” Considering the associated Sturm–Liouville problem, he has developed a method which leads to well-posed numerical solutions.

For the Bessel horns (iv), noting  $P(\ell, \omega)$  the Fourier transform of  $\tilde{p}(\ell, t)$ , the corresponding wave equation is

$$\partial_\ell^2 P(\ell, \omega) + \frac{2\alpha}{\ell} \partial_\ell P(\ell, \omega) + \frac{\omega^2}{c^2} P(\ell, \omega) = 0, \quad (61)$$

so that solutions take the form

$$P(\ell, \omega) = P_0(\omega) \ell^{1/2-\alpha} J_{\alpha-1/2} \left( \frac{\ell \omega}{c} \right) + P_1(\omega) \ell^{1/2-\alpha} Y_{\alpha-1/2} \left( \frac{\ell \omega}{c} \right), \quad (62)$$

TABLE II. This table sums up for the cases (i)–(iv) the expression of  $F$  used to compute  $\mathcal{R}'$  from  $\mathcal{R}$ , and the minimum [(iii),(iv)  $0 < \alpha < 1$ ] or maximum [(i),(ii),(iv)  $\alpha \in [0, 1]$ ] radius  $R^*$  for which an infinite slope is reached on the physical shape.

Case	$F(R)$	$R^*$
(i) $\alpha > 0$	$\alpha R$	$\alpha^{-1}$
(ii) $\alpha > 0$	$\alpha \sqrt{R^2 - R_0^2}$	$\sqrt{R_0^2 + \alpha^{-2}}$
(iii) $\alpha > 0$	$\alpha \sqrt{R_0^2 - R^2}$	$\sqrt{R_0^2 - \alpha^{-2}}$ if $ \alpha R_0  \geq 1$
(iv) $\alpha \neq 0 \ \alpha \neq 1$	$\alpha R_0^{(1/\alpha)} R^{(\alpha-1)/\alpha}$	$R_0^{1/(1-\alpha)}  \alpha ^{1/(1-\alpha)}$

where  $J_\nu$  and  $Y_\nu$  are the Bessel functions of the first and the second kind<sup>16</sup> (Chap. 9), respectively, and  $P_0, P_1$  are arbitrary.

Nevertheless, such profiles are known when the Webster equation is written for the variable  $z$  rather than  $\ell$ . Thus, although analytical results are unchanged for the pressure resolution, that is not the case for the real physical shapes. In particular, the new computed profiles have an unusual characteristic: for some of them, their radius or their length is required to be bounded.

## 2. Properties of physical shapes

Let  $z \mapsto L(z)$  be the length of the wall  $\mathcal{W}$  from  $z_0 = 0$  to  $z$ , defined by Eq. (56). Differentiating the expression  $R(z) = \mathcal{R}(L(z))$  gives

$$\mathcal{R}'(L(z)) = \frac{R'(z)}{\sqrt{1 + R'(z)^2}}. \quad (63)$$

This implies that  $|\mathcal{R}'| \leq 1$ , the limit case  $|\mathcal{R}'| = 1$  corresponding to an infinite slope for the physical shape. Except for the sinusoidal profile when  $|\alpha R_0| < 1$ , the formula  $\mathcal{R}(\ell)$  remains physically meaningful only on lower- or upper-bounded intervals so that a maximum or minimum radius  $R^*$  associated with a length  $\ell^*$  may be defined (see Table II).

Note that if a  $\mathcal{C}^1$ -regular profile ends with a slope  $\mathcal{R}' = 1$  at  $\ell = \ell^*$ , prolonging the profile by the cone defined by  $\mathcal{R}'(\ell) = 1$  for  $\ell \geq \ell^*$  corresponds to a baffled pipe. This profile still satisfies the  $\mathcal{C}^1$ -regularity. In this case, Eq. (55) implies that, for  $\ell \geq \ell^*$ , the pressure propagates as spherical waves.

## 3. Computation of physical shapes

The computation of  $R(z)$  from  $\mathcal{R}(\ell)$  can be achieved in an implicit way if there exists an  $F$  such that  $\mathcal{R}' = F(\mathcal{R})$ . In this case, Eq. (63) yields

$$\frac{R'(z)}{\sqrt{1 + R'(z)^2}} = F(\mathcal{R}(L(z))) = F(R(z))$$

which is proven equivalent to

$$\frac{F(R(z))}{\sqrt{1 - F(R(z))^2}} R'(z) = 1. \quad (64)$$

If  $z \mapsto F(R(z))/\sqrt{1 - F(R(z))^2}$  is bijective, the integration of Eq. (64) from  $z_0$  to  $z$  may be written

$$\int_{R(z_0)}^{R(z)} \frac{F(r)}{\sqrt{1 - F(r)^2}} dr = z, \quad (65)$$

which solves  $z$  as a function of the radius. The functions  $F$  associated with the shapes (i)–(iv) are specified in Table II. The geometrical differences between these profiles drawn for both  $z$  and  $\ell$  may be assessed in Fig. 5. Note that this figure exhibits the maximum and minimum radii.

## V. GENERALIZATION FOR SMALL WALL ADMITTANCES AND MOBILE WALLS

When the wall  $\mathcal{W}_t$  is mobile or is not ideally rigid and lossless, the normal component of the acoustic velocity is no longer zero. Nevertheless, the wall  $\mathcal{W}_t$  may still be described by  $\mathcal{T}_{w,t}$  for a constant  $u = w$ , and the general notations Eq. (38) to Eqs. (40) remain valid. The only differences are that  $f|_w$  and  $g|_w$  may be time-varying and that  $\epsilon|_w \neq 0$  since the wall condition  $(\tilde{\mathbf{v}} \cdot \mathbf{w}_s|_w \neq 0)$  prevents isobars from being orthogonal to  $\mathcal{W}_t$ . In this case, the boundary conditions on  $\mathcal{W}_t$  may be described by a relation linking  $\tilde{p}$  and  $\tilde{\mathbf{v}} \cdot \mathbf{w}_s|_w$ . Such a relation is usually specified in the Fourier domain using a *wall admittance*  $Y$ .

As an example, if a quasiplanar wall is vibrating, a standard boundary condition is described for  $u = w$  by<sup>17</sup> (p. 47)

$$\partial_{\mathbf{w}_s} \hat{p} + \frac{i\omega}{c} Y(\omega) \hat{p} = -i\omega \rho_0 \hat{\mathbf{V}} \cdot \mathbf{w}_s, \quad (66)$$

where  $\partial_{\mathbf{w}_s} = \mathbf{w}_s \cdot \text{grad}$  is the derivative in the direction  $\mathbf{w}_s$ ,  $Q \mapsto \hat{Q}$  gives the Fourier transform defined for the angular frequency  $\omega$ , and  $\mathbf{V}$  is the local velocity of  $\mathcal{W}_t$ .  $Y = \rho_0 c [\mathbf{w}_s \cdot (\hat{\mathbf{v}} - \hat{\mathbf{V}})]|_w / \hat{p}$  is the specific admittance of the material constituting the wall. Note that  $Y$  is ordinarily given such that  $\mathbf{w}_s$  is outwardly directed, so that particular attention must be paid to the conventions used. This direction is achieved choosing  $g|_w \geq 0$  and  $f|_w$  such that the inside of the guide is at the right-hand side of  $\mathbf{u}_s$ .

This section establishes a mono-space wave equation in this general context for cases such that  $\epsilon|_w \ll 1$ , making  $\epsilon^2|_w$  and  $\epsilon^3|_w$  negligible. This restriction still encompasses many physical cases for which the wall admittance and thus  $\partial_{\mathbf{w}_s} \tilde{p}|_w$  are small, as clarified below by Eq. (67). The reason for this restriction is also detailed.

### A. Derivation of the 1D model

Establishing a 1D model from Eq. (20) requires coping with two problems. The first one consists of making the boundary condition usable, showing a relation between  $\epsilon|_w$  and  $\partial_{\mathbf{w}_s} \tilde{p}$ . This stage stands in for the simplification run in Sec. IV considering that  $\epsilon = 0$ . Projecting Eq. (19) on  $\mathbf{w}_s$  leads to this requisite identification given by

$$\epsilon = \sigma_s \frac{\partial_{\mathbf{w}_s} \tilde{p}}{\partial_s \tilde{p}}. \quad (67)$$

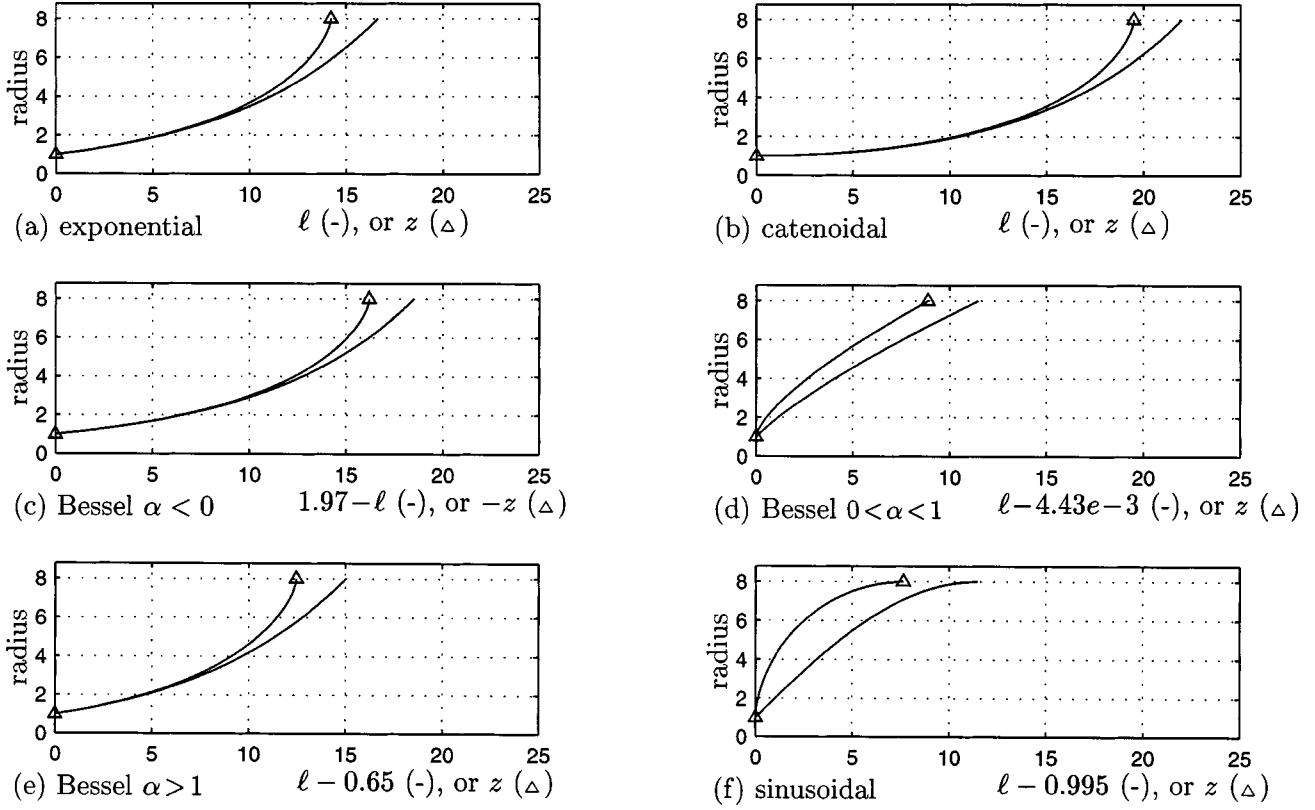


FIG. 5. The profiles corresponding to the cases (i)–(iv) are drawn for both the  $\ell$ -ordinate (—), and the  $z$ -ordinate ( $\Delta$ ). Parameters are computed so that  $R^*$  is reached,  $R_{\min}=1$  unit, and  $R_{\max}=8$  units: (a)  $R_0=1$ ,  $\alpha=1/8$ , (b)  $R_0=1$ ,  $\alpha=1/\sqrt{63}$ , (c)  $R_0\approx 8.6e-3$ ,  $\alpha=-10$ , (d)  $R_0\approx 0.381$ ,  $\alpha\approx 0.743$  [computed to have the same length for (d) and (f)], (e)  $R_0\approx 0.745$ ,  $\alpha=10$ , (f)  $R_0=8$ ,  $\alpha=1/\sqrt{63}$ . Appropriate translations in  $\ell$  [and a symmetry for (c)] are used to make the profiles increasing and starting at  $\ell=z=0$ .

The main remaining problem is the evaluation of  $\partial_u \phi / (\sigma_u \cos \delta)$  on  $\mathcal{W}_t$ . Once again, the local quasisphericity of isobars near the wall makes the solution of the propagation problem separate from that of the geometry of isobars. Actually, this hypothesis is obtained as in Sec. IV B. The only noteworthy differences are that a point  $M(s, t)$  of  $\mathcal{W}_t$  indexed by  $s$  can be nonstationary, and that  $\epsilon|_w$  is not required to be zero. Nevertheless, all the definitions and the calculations [Eqs. (41)–(50)] remain exact, adapting the notations as illustrated in Fig. 6, and considering  $O_{s,t}$ ,  $z_{O_{s,t}}$ ,  $R_{s,t}$  in place of  $O_s$ ,  $z_{O_s}$ , and  $R_s$  in the previous formula.

Then, recalling that  $\delta = \phi - \theta$ , Eq. (50) yields

$$\left. \frac{\partial_u \phi}{\sigma_u \cos \delta} \right|_w = \left. \frac{\cos \theta + \epsilon \sin \theta}{g} \right|_w. \quad (68)$$

Using Eq. (67) and neglecting  $\epsilon^2$  and  $\epsilon^3$  in  $A_{s,s}$  and  $A_s$ , the hypothesis of quasisphericity Eq. (68) leads to

$$\begin{aligned} B_{s,s} \partial_s^2 \tilde{p} + B_s \partial_s \tilde{p} + B_{s,t} \partial_s \partial_t \tilde{p} - \frac{1}{c^2} \partial_t^2 \tilde{p} + B_{w_s} \partial_{w_s} \tilde{p} \\ + B_{w_{s,s}} \partial_s \partial_{w_s} \tilde{p} + B_{w_{s,t}} \partial_t \partial_{w_s} \tilde{p} = 0, \end{aligned} \quad (69)$$

where

$$B_{s,s} = (1 - \xi_s^2) / \sigma_s^2, \quad (70a)$$

$$\begin{aligned} B_s = \frac{2 - \xi_n^2}{\sigma_s^2} \partial_s \ln g - \frac{1 - \xi_n^2}{\sigma_s^2} \partial_s \ln \sigma_s \\ - \frac{1}{2} \partial_s \left( \frac{\xi_s^2 - \xi_n^2}{\sigma_s^2} \right) + \frac{1}{c} \partial_t \left( \frac{\xi_s}{\sigma_s} \right), \end{aligned} \quad (70b)$$

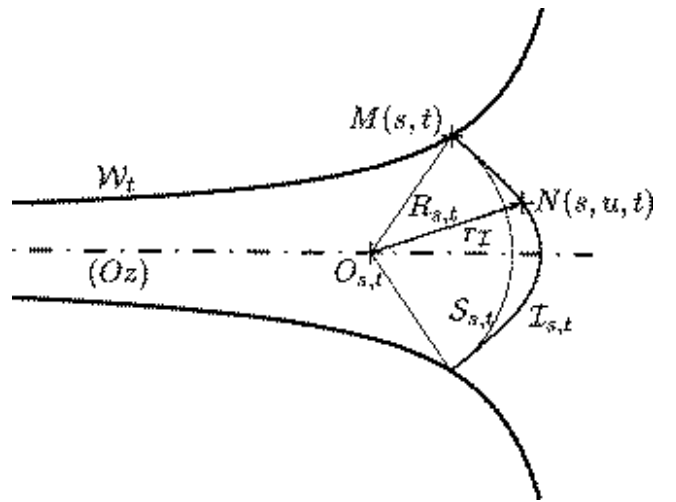


FIG. 6. When the wall is not rigid, motionless, or lossless, isobars are not necessarily orthogonal to the wall. The hypothesis of their quasisphericity near the wall can still be considered in this more general case. Note that the spheres  $\mathcal{S}_{s,t}$  tangent to isobars  $\mathcal{I}_{s,t}$  now move with respect to the angle  $\phi(s, w, t)$  which is no longer a right angle. Nevertheless, the formula of definition Eq. (41) to Eq. (50) are not modified: the only differences are that  $O_s$ ,  $z_{O_s}$ , and  $R_s$  may now depend on the time.



$$B_{s,t} = 2 \frac{\xi_s}{c \sigma_s}, \quad (70c)$$

$$B_{\mathbf{w}_s} = \frac{2 - \xi_n^2}{g} \cos \theta + \frac{1 - 2\xi_n^2}{\sigma_s} \partial_s \theta - \frac{\xi_s}{\sigma_s} \partial_s \xi_n + \frac{1}{c} \partial_t \xi_n, \quad (70d)$$

$$B_{\mathbf{w}_{s,s}} = -2 \xi_s \xi_n / \sigma_s, \quad (70e)$$

$$B_{\mathbf{w}_{s,t}} = 2 \xi_n / c, \quad (70f)$$

are all evaluated for  $u=w$ . Finally, Eq. (69) and boundary conditions such as Eq. (66) furnish a 1D model of the waveguide. As analyzed in Sec. IVD, the validity of this 1D model is still limited to walls having a small curvature. This assumption holds only if  $\partial_s \theta|_w$  is negligible. Practically,  $B_{\mathbf{w}_s}$  is well approximated by

$$B_{\mathbf{w}_s} = \frac{2 - \xi_n^2}{g} \cos \theta - \frac{\xi_s}{\sigma_s} \partial_s \xi_n + \frac{1}{c} \partial_t \xi_n. \quad (71)$$

Particular derivations for visco-thermal losses on the wall or for mobile walls are described below. Beforehand, the requirement  $\epsilon|_w \ll 1$  is clarified.

## B. Geometrical hypothesis and compatibility with the problem

Let  $\mathcal{P}$  describe the problem associated with the propagation in a given waveguide for which the wall conditions are linear with respect to the pressure. The linearity of the wave equation Eq. (3) and of the wall conditions ensures that of the acoustic propagation in the guide. Consequently, for such conditions, the exactness of the establishment of Eq. (20) and Eq. (67) guarantees the preservation of this property. However, if  $\tilde{p}_1$  and  $\tilde{p}_2$  are two solutions of these equations,  $\tilde{p} = \tilde{p}_1 + \lambda \tilde{p}_2$  does not appear as an obvious solution. Only  $\lambda \tilde{p}_1$  or  $\lambda \tilde{p}_2$  appears obvious when the motion of  $\mathcal{W}_t$  is imposed. These particular properties are now described and investigated.

Under the linearity assumption of the wall conditions, the operator  $\tilde{p} \mapsto \lambda \tilde{p}$  keeps  $\epsilon$  invariant [see Eq. (67)]. It then acts on the first member of Eq. (20) as a multiplication by  $\lambda$  (first-order homogeneity) for imposed  $\xi_s$  and  $\xi_n$ . This proves that, for any solution  $\tilde{p}$  of a problem  $\mathcal{P}$ ,  $\lambda \tilde{p}$  is also a solution. On the contrary, making the operator  $(\tilde{p}_1, \tilde{p}_2) \mapsto \tilde{p}_1 + \lambda \tilde{p}_2$  act on Eq. (20) and Eq. (67) does not lead to such relations. This is not a paradox but is simply due to the writing of  $\mathcal{P}$  in the isobaric coordinate system. This indicates that the inherent linearity of  $\mathcal{P}$  explicitly involves the coupling between the propagation and the geometry of isobars: multiplying a solution pressure by  $\lambda$  does not change the isobaric map, but another change of solution does. More precisely, it gives information about  $\partial_u \phi / \sigma_u$  for which the compatibility with the quasisphericity hypothesis requires study.

Starting from Eq. (20) and Eq. (67), the exact wave equation for the problem  $\mathcal{P}$  may be written as the nullity of the sum of three terms  $T_{ne}[\tilde{p}]$ ,  $T_{nl}[\tilde{p}]$ , and  $T_l[\tilde{p}]$  defined below.  $T_{ne}[\tilde{p}]$  corresponds to the term of Eq. (20) which is

not evaluable for  $u=w$  from the single geometry of the wall. It corresponds to

$$T_{ne}[\tilde{p}] = (1 - \xi_n^2) \left[ 1 + \left( \frac{\sigma_s \partial_{\mathbf{w}_s} \tilde{p}}{\partial_s \tilde{p}} \right)^2 \right] \frac{\partial_u \phi}{\sigma_u \cos \delta} \frac{\partial_s \tilde{p}}{\sigma_s}, \quad (72)$$

for which it is recalled that  $\partial_u \phi / \sigma_u$  is the only quantity non-evaluable on  $\mathcal{W}_t$ , and where  $\cos \delta$  is not developed using  $\partial_{\mathbf{w}_s} \tilde{p}$  and  $\partial_{\mathbf{u}_s} \tilde{p}$  to keep the formula compact.  $T_{nl}[\tilde{p}]$  contains all other terms which are nonlinear in  $\epsilon$ , and is given by

$$T_{nl}[\tilde{p}] = (1 - \xi_n^2) \left[ \left( \frac{\partial_{\mathbf{w}_s} \tilde{p}}{\partial_s \tilde{p}} \right)^2 (\sigma_s \partial_s \theta \partial_{\mathbf{w}_s} \tilde{p} + \partial_s \ln \sigma_s \partial_s \tilde{p} - \partial_s^2 \tilde{p}) + 2 \frac{\partial_{\mathbf{w}_s} \tilde{p}}{\partial_s \tilde{p}} \partial_s \partial_{\mathbf{w}_s} \tilde{p} \right]. \quad (73)$$

The remaining term  $T_l[\tilde{p}]$  is constituted only of linear terms evaluable for  $u=w$ : all the first-order terms such as  $-2 \xi_n \xi_s \epsilon \partial_s^2 \tilde{p} / \sigma_s^2$  in  $A_{s,s}$ , or  $2 \xi_n \epsilon \partial_s \partial_t \tilde{p} / (c \sigma_s)$  in  $A_{s,t}$ , vanish with those of  $A_s$  when expressing  $\epsilon$  thanks to Eq. (67).  $T_l[\tilde{p}]$  would correspond exactly to the first member of Eq. (69) omitting the contribution in  $B_s$  and  $B_{\mathbf{w}_s}$  of  $T_{ne}$  after using the quasisphericity hypothesis.

Defining  $T[\tilde{p}] = T_{ne}[\tilde{p}] + T_{nl}[\tilde{p}] + T_l[\tilde{p}]$ , the wave equation is obtained writing  $T[\tilde{p}] = 0$ . The condition of linearity is then obtained writing

$$T[\tilde{p}_1 + \lambda \tilde{p}_2] = T[\tilde{p}_1] + \lambda T[\tilde{p}_2], \quad (74)$$

for all  $\tilde{p}_1$  and  $\tilde{p}_2$  solutions, and for all  $\lambda$ . When  $\xi_s$  and  $\xi_n$  are unchanged for distinct solutions (for instance, rigid but controlled mobile walls),  $T_l$  is linear so that this condition is reduced to Eq. (74) taking  $T[\tilde{p}] = (T_{ne}[\tilde{p}] + T_{nl}[\tilde{p}]) / (1 - \xi_n^2)$ . Equation (74) exhibits the nonlinear relation between the three geometrical coefficients  $(\partial_u \phi / \sigma_u)_P$  associated with the problem  $\mathcal{P}$  for the pressures  $\tilde{p} = \tilde{p}_1$ ,  $\tilde{p}_2$ ,  $\tilde{p}_1 + \lambda \tilde{p}_2$ , and these three pressures.

The quasisphericity hypothesis does not mostly satisfy this condition since it makes  $(\partial_u \phi / \sigma_u)|_w$  depend only on the wall geometry but not on the pressure. As a consequence, the linearity of the 1D model for this hypothesis requires  $\epsilon|_w \ll 1$ , so that the induced nonlinear terms may be neglected, leading to Eq. (69).

## C. Influence of mobile walls

Equation (69) can be straightforwardly used to establish a 1D model for a controlled mobile wall.

From Eq. (10a) and Eq. (11a), the time derivatives of  $\mathbf{u}_s$  and  $\mathbf{w}_s$  are obtained for

$$\partial_t \mathbf{u}_s = \partial_t \theta \mathbf{w}_s, \quad (75a)$$

$$\partial_t \mathbf{w}_s = -\partial_t \theta \mathbf{u}_s. \quad (75b)$$

Since from Eqs. (14),  $\mathbf{V}/c = \xi_s \mathbf{u}_s + \xi_n \mathbf{w}_s$ , the acceleration  $\partial_t \mathbf{V}$  is such that

$$\partial_t \left( \frac{\mathbf{V}}{c} \right) = (\partial_t \xi_s - \xi_n \partial_t \theta) \mathbf{u}_s + (\partial_t \xi_n + \xi_s \partial_t \theta) \mathbf{w}_s. \quad (76)$$

As  $\partial_{\mathbf{w}_s} \tilde{p} = \mathbf{w}_s \cdot \text{grad}(\tilde{p})$ , Eq. (2) and Eq. (76) yields

$$\partial_{\mathbf{w}_s} \tilde{p} = -\rho_0 c (\partial_t \xi_n + \xi_s \partial_t \theta). \quad (77)$$

Equation (77), evaluated on the wall, and Eq. (69) furnish the 1D model.

Note that the hypotheses involved to linearize the Navier–Stokes equations and used to derive Eq. (3) require that  $\xi_s \ll 1$  and  $\xi_n \ll 1$ , so that terms of high order in  $\xi_s$  or  $\xi_n$  may be neglected. Describing  $\mathbf{W}_t$  with  $\mathcal{R}(\ell, t) = g|_w(\ell, t)$ ,  $\ell$  being the curvilinear ordinate such that  $\sigma_s|_w(\ell, t) = 1$ , the model takes a simpler form

$$\begin{aligned} \partial_{\ell}^2 \tilde{p} + \left( 2 \frac{\partial_{\ell} \mathcal{R}}{\mathcal{R}} + \frac{\partial_t \xi_s}{c} \right) \partial_{\ell} \tilde{p} + 2 \frac{\xi_s}{c} \partial_t \partial_{\ell} \tilde{p} - \frac{1}{c^2} \partial_t^2 \tilde{p} \\ = \rho_0 c \left[ \left( \frac{2 \cos \theta}{\mathcal{R}} + \frac{\partial_t \xi_n}{c} \right) + 2 \frac{\xi_n}{c} \partial_t \right] (\partial_t \xi_n + \xi_s \partial_t \theta), \end{aligned} \quad (78)$$

where the geometrical quantities are still evaluated for  $u = w$  and the second member may be interpreted as sources induced by the motion of  $\mathbf{W}_t$ .

For many practical cases, the controlled motion or the vibrations of the wall are sufficiently small to consider much stronger approximations so that Eq. (78) can be reduced to

$$\partial_{\ell}^2 \tilde{p} + 2 \frac{\partial_{\ell} \mathcal{R}}{\mathcal{R}} \partial_{\ell} \tilde{p} - \frac{1}{c^2} \partial_t^2 \tilde{p} = \rho_0 c \frac{2 \cos \theta}{\mathcal{R}} (\partial_t \xi_n + \xi_s \partial_t \theta), \quad (79)$$

for  $u = w$ . For vibrating walls, this last acoustic equation may be coupled with the model of the wall vibrations.

## D. Influence of visco-thermal losses

Equation (69) also enables treating the case of a pipe with visco-thermal losses due to the wall, now assumed motionless. The radius of the pipe is assumed to be large in relation to the boundary-layer thickness, but small compared to the wavelength.

Let significant parameters specifying the properties and the nature of the fluid at rest be defined: the coefficient of shear viscosity  $\mu$ , the coefficient of thermal conductivity  $\lambda$ , the heat coefficients at constant pressure and constant volume per unit of mass  $C_P$  and  $C_V$ , the specific heat ratio  $\gamma = C_P/C_V$ , and finally the characteristic lengths  $l'_v = \mu/(\rho_0 c)$  and  $l_h = \lambda/(\rho_0 c C_P)$ . The effect of the visco-thermal losses on the acoustics may be described for travelling waves by an equivalent specific wall admittance  $Y$  given by<sup>17</sup> (pp. 112–115)

$$Y(\omega, s) = \left( \frac{i\omega}{c} \right)^{1/2} [\kappa(s) \sqrt{l'_v} + (\gamma - 1) \sqrt{l_h}], \quad (80)$$

where  $\kappa$  is linked to the angle of incidence of the wavefronts on  $\mathbf{W}_t$  as described below. Note that to be physically meaningful,  $Y$  must have an Hermitian symmetry so that the complex  $(i\omega)^{1/2}$  needs to be specified: this quantity may be understood as  $\sqrt{|\omega|} \exp(i\pi/4)$  for  $\omega \geq 0$ , and the conjugate  $\sqrt{|\omega|} \exp(-i\pi/4)$  for  $\omega < 0$ . More precisely, this definition makes it correspond to the time operator  $\partial_t^{1/2}$  for causal functions.<sup>18</sup>

The validity of Eq. (80) relies on the fact that the thickness of the boundary layer must be very small with regard to

both the radius and the radius of curvature of  $\mathbf{W}$ . For a pulsation  $\omega$ , the thickness is given by  $\sqrt{2cl'_v/\omega}$  for the viscous effects, and  $\sqrt{2cl_h/\omega}$  for the thermal effects. For usual conditions,  $l'_v$  and  $l_h$  are about  $4 \times 10^{-8}$  m and  $6 \times 10^{-8}$  m so that the thermal effects are the most restrictive. The thickness decreases with the frequency  $f$  as  $f^{-1/2}$  and is about 2.5 mm at  $f = 1$  Hz for the thermal effects. This condition is then fulfilled for many practical cases.

Now,  $\kappa(s)$  corresponds to the square of the sine of the angle<sup>17</sup> (p. 155)  $[\mathbf{u}_s, \mathbf{grad}(\tilde{p})]$ , or identically, to  $\cos^2 \delta = 1/(1 - \epsilon^2)$ . As  $\epsilon^2$  is neglected above,  $\kappa$  may be approximated by 1. Then, if  $\mathbf{w}_s$  is outwardly directed, the boundary condition Eq. (66) (for  $\mathbf{V} = \mathbf{0}$ ) is written in the time domain by

$$\partial_{\mathbf{w}_s} \tilde{p} + \frac{\sqrt{l'_v} + (\gamma - 1) \sqrt{l_h}}{c^{3/2}} \partial_t^{3/2} \tilde{p} = 0, \quad (81)$$

where for usual conditions  $\sqrt{l'_v} + (\gamma - 1) \sqrt{l_h}$  is about  $3 \times 10^{-4} \text{ m}^{1/2}$ . This order of magnitude confirms that the effect due to the boundary layer is small so that the assumption  $\epsilon \ll 1$  is well founded in this case, and the quasisphericity hypothesis is compatible with the problem.

Finally, the dominating practical requirement is the slowness of the variation of the cross section of the pipe. The 1D model obtained for these pipes from Eq. (69) and Eq. (81) with  $\xi_s|_w = \xi_n|_w = 0$  is given for  $u = w$  by

$$\frac{1}{\sigma_s^2} \partial_s^2 \tilde{p} + \frac{2 \partial_s \ln g}{\sigma_s^2} \partial_s \tilde{p} - \frac{1}{c^2} \partial_t^2 \tilde{p} - \frac{2 \cos \theta}{g} \frac{\Gamma}{c^{3/2}} \partial_t^{3/2} \tilde{p} = 0, \quad (82)$$

where  $\Gamma = \sqrt{l'_v} + (\gamma - 1) \sqrt{l_h}$ . For the ordinate  $\ell$  for which  $\sigma_s|_w = 1$ , this equation appears as a Webster equation perturbed by the low fractional differential term  $2(\cos \theta/(c^{3/2} g)) \Gamma \partial_t^{3/2} \tilde{p}$ . Note that for the profile  $g|_w(s) = R_0$ , this equation exactly yields the well-known equation of plane waves guided in cylindrical tubes with visco-thermal losses<sup>17</sup> (p. 145).

## VI. CONCLUSION

A rigorous derivation of the linear acoustic wave equation in any local isobaric coordinate system has been presented for axisymmetric problems. As the main theoretical result of this work, it formally demonstrates the exact coupling between the geometry of the isobars and the propagation of the pressure. Straightforward derivations have shown that any regular isobaric map may satisfy a purely geometrical criterion of admissibility. The general static isobaric maps have been proven to be parallel planes, coaxial cylinders, and concentric spheres. Other static maps exist but, in this case, only a pure sinusoid or a pure exponential can travel on each of them. Furthermore, the isobaric wave equation shows that separating the resolution of the isobaric map from that of the 1D pressure is usually impossible. Assuming the quasisphericity near the wall for a minimal order is proven to be sufficient to dispose of this problem. The 1D models derived for motionless rigid walls or mobile ones with small admittances constitute the second main result of

this work. They make the arc length of the wall appear as the natural distance travelled by a wave with the speed  $c$ .

The interests are to draw benefit from the low computational cost of 1D models, and to improve the quality, thanks to a prior, quite complex differential calculus and a geometrical hypothesis which is weaker than usual. A spatial resolution for the 1D models having motionless walls yields a representation with input–output systems that are not expensive to simulate<sup>19</sup> and make real-time applications possible.

Even if the geometrical hypothesis does not require fixed wavefronts as usual, the limitations mostly remain those of the classical Webster equation, namely, smooth wall contours with low curvature, and sufficiently large wavelengths ensuring that transverse modes are not excited. To quantify the quality of the 1D models, a numerical validation will be run comparing the pressure deduced for them to that computed near the wall with the PAK algorithm,<sup>10,11</sup> but also with finite-element methods. In particular, the horns presented in Sec. IV E could be tested for an excitation  $\tilde{p}(0,t)$  at the input  $s=0$  and for a given load admittance at the output  $s=L$  such as that of divergent spherical waves. For the 2D algorithms, the same boundary conditions may be taken on the spheres orthogonal to the wall in  $s=0$  and  $s=L$ , the quasisphericity hypothesis being appropriate to this geometry. Other meaningful comparisons with 2D models may be done for boundary conditions which are compatible with the quasisphericity hypothesis and adaptable to 1D models [e.g., radiating portion of a sphere<sup>17</sup> (p. 246)].

Nevertheless, whatever the success of a numerical validation, this work can be expanded to other models having a mono-spatial dependence, which would exceed the above-mentioned limitations. Indeed, starting from the general rigorous Eq. (20), geometrical hypotheses more relaxed than that of quasisphericity could be used. Mainly, choosing hypotheses of higher orders is an interesting prospect. A particularly interesting one is an order of regularity and of flexibility imposed on the wavefront geometry by  $\partial_{\mathbf{u}}^K \phi|_w = 0$  [with  $\partial_{\mathbf{u}} = (1/\sigma_u)\partial_u$ ] for a given  $K \geq 2$  ( $K=0$  would impose the wrong angle  $\phi|_w = 0$ , and  $K=1$  would impose quasiplanar wavefronts near the wall rather than the more appropriate quasispherical ones). But such alternatives will involve extensive investigation. Indeed, establishing the associated 1D models requires solving the system of equations obtained by applying  $X \mapsto \partial_{\mathbf{u}}^k X|_w$  on Eq. (20) for  $k=0,1,\dots,K-1$ , the hypothesis being used in the last equation. A careful study of fundamental properties such as the linearity or the compatibility with the symmetry of the problem must be performed since they are not guaranteed *a priori*. In addition to the relaxation of the above-mentioned constraints induced by the quasisphericity hypothesis, the main interest of this extension is potentially having control of the input–output isobar geometry through the integrating constants linked to  $\partial_{\mathbf{u}}^k \phi|_w$ . In this case, the corresponding 1D models account for the propagation of the pressure as well as that of the geometrical information represented.

## ACKNOWLEDGMENTS

The research reported here is based on a doctoral dissertation completed by the author at the University of Paris XI-Orsay. The author thanks X. Rodet, the Analysis–Synthesis team at IRCAM, and the Ministry of Research for supporting this research. The author is very grateful to J. Kergomard and C. Vergez for their critical reading of this paper, as well as S. Mac Adams and M. Lo Cascio for proof-reading this paper before submission to the Journal of the Acoustical Society of America.

- <sup>1</sup>D. Bernoulli, “Sur le son et sur les tons des tuyaux d’orgues différemment construits” (Physical, Mechanical and Analytical Researches on Sound and on the Tones of Differently Constructed Organ Pipes), Mém. Acad. Sci. (Paris), 1764 [in French, reference extracted from the paper of Eisner (Ref. 4)].
- <sup>2</sup>J. L. Lagrange, “Nouvelles recherches sur la nature et la propagation du son” (New Researches on the Nature and Propagation of Sound), Misc. Taurinensia (Mélanges Phil. Math., Soc. Roy. Turin), 1760–1761 [in French, reference extracted from the paper of Eisner (Ref. 4)].
- <sup>3</sup>A. G. Webster, “Acoustical impedance, and the theory of horns and of the phonograph,” Proc. Natl. Acad. Sci. U.S.A. **5**, 275–282 (1919); **6**, 320(E) (1920).
- <sup>4</sup>E. Eisner, “Complete solutions of the “Webster” horn equation,” J. Acoust. Soc. Am. **41**, 1126–1146 (1967).
- <sup>5</sup>R. F. Lambert, “Acoustical studies of the tractrix horn. I,” J. Acoust. Soc. Am. **26**, 1024–1028 (1954).
- <sup>6</sup>E. S. Weibel, “On Webster’s horn equation,” J. Acoust. Soc. Am. **27**, 726–727 (1955).
- <sup>7</sup>A. H. Benade and E. V. Jansson, “On plane and spherical waves in horns with nonuniform flare. I. Theory of radiation, resonance frequencies, and mode conversion,” Acustica **31**, 79–98 (1974).
- <sup>8</sup>G. R. Putland, “Every one-parameter acoustic field obeys Webster’s horn equation,” J. Audio Eng. Soc. **6**, 435–451 (1993).
- <sup>9</sup>A. F. Stevenson, “Exact and approximate equations for wave propagation in acoustic horns,” J. Appl. Phys. **22**(12), 1461–1463 (1951).
- <sup>10</sup>V. Pagneux, N. Amir, and J. Kergomard, “A study of wave propagation in varying cross-section waveguides by modal decomposition. Part I. Theory and validation,” J. Acoust. Soc. Am. **100**, 2034–2048 (1996).
- <sup>11</sup>J. A. Kemp, “Theoretical and experimental study of wave propagation in brass musical instruments,” Ph.D. thesis, Edinburgh University, 2002.
- <sup>12</sup>J. Agulló, A. Barjau, and D. H. Keefe, “Acoustic propagation in flaring, axisymmetric horns: I. A new family of unidimensional solutions,” Acustica **85**, 278–284 (1999).
- <sup>13</sup>P. M. Morse and K. U. Ingard, *Theoretical Acoustics* (McGraw-Hill, New York, 1968).
- <sup>14</sup>*Field Theory Handbook, Including Coordinate Systems, Differential Equations and their Solutions*, 2nd ed. (1971) corrected 3rd printing (1988) (Springer-Verlag, New York, Heidelberg, Berlin, 1988), pp. 34–36.
- <sup>15</sup>D. P. Berners, “Acoustics and signal processing techniques for physical modeling of brass instruments,” Ph.D. thesis, Stanford University, 1999.
- <sup>16</sup>*Handbook of Mathematical Functions*, edited by M. Abramowitz and I. A. Stegun (Dover, New York, 1970).
- <sup>17</sup>M. Bruneau, *Manuel d’acoustique fondamentale (Manual of fundamental acoustics), Etudes en mécanique des matériaux et des structures (Studies in the mechanics of materials and structures)* (Hermès, Éditions Hermès, Paris, France, 1998).
- <sup>18</sup>D. Matignon, “Stability properties for generalized fractional differential systems,” ESAIM Proc. **5**, 145–158 (1998) (available on the World Wide Web).
- <sup>19</sup>T. Hélie, “Modélisation physique des instruments de musique en systèmes dynamiques et inversion (Physical modeling of musical instruments with dynamic systems and inversion processes),” Ph.D. thesis, Université de Paris XI-Orsay, IRCAM-Centre Georges Pompidou, Paris, 2002.